30

DENDRITIC POLYMERS

Jason Dockendorff and Mario Gauthier

30.1 INTRODUCTION

Dendritic species represent the most recently discovered class of branched macromolecular architecture. Major developments in linear, crosslinked, and branched architectures date back roughly to the 1930s, 1940s, and 1960s, respectively. The first synthetic dendritic species were reported in 1978 [1]; however, much of the work in this area began to build momentum only in the mid-1980s. A chronology of the key developments in dendritic polymers is provided in Table 30.1.

Dendritic patterns can be found all around us in nature and within us. The drainage pattern of rivers and their tributaries, plant roots and foliage, and neurons within our body are but a few examples of unique branched systems ranging in size from kilometers down to micrometers. Molecular dendritic species recreate fractal-like patterns on the nanometric scale. Dendritic macromolecules can be divided into three subclasses on the basis of their structural characteristics: dendrimers, hyperbranched polymers, and dendrigraft polymers (including arborescent polymers). Dendrimers should ideally have a perfect branched structure, hyperbranched polymers rely on statistical branching giving a highly imperfect structure, while the architecture of dendrigraft polymers is best described as semi-controlled. A second subclass of controlled structures is the dendrons, which are dendritic fragments formed by a monofunctional initiator or core.

A graphical comparison of the structure of dendrons, dendrimers, hyperbranched polymers, and dendrigraft polymers is shown in Figure 30.1. The stepwise synthesis of dendrimers involves multiple cycles of protection, condensation, and deprotection reactions to produce strictly controlled branched structures and extremely narrow molecular weight distributions (MWD): the molecular weight dispersity ($Đ = M_w/M_n$) attained for such molecules can be less than 1.01. The preparation of dendrigraft polymers also relies on stepwise, generation-based synthetic procedures but uses polymeric building blocks rather than small molecules and branching points randomly distributed on the coupling substrate. Under appropriate reaction conditions, usually involving ionic polymerization and grafting, low molecular weight dispersities can also be achieved for these systems ($Đ \approx 1.05-1.10$). The completely random branching process used in the synthesis of hyperbranched polymers, typically resulting from the condensation of nonprotected polyfunctional monomers, provides the least defined structures, a $Đ > 2$ being obtained in most cases.

Each color in Figure 30.1 represents the branching levels derived from building blocks introduced in successive generations, these being small molecules for dendrons, dendrimers, and hyperbranched polymers (Fig. 30.1a–c), and polymeric segments for the dendrigraft polymers (Fig. 30.1d). Dendrons are closely related to the dendrimers of Figure 30.1b, the main distinction being the number of functional groups available on the substrate serving as core in the first reaction step. It should also be noted that hyperbranched polymers can be obtained from polymeric segments (e.g., macromonomers) as well as small molecules.

Dendritic macromolecules constructed from small-molecule monomers incorporate three major components: a core, repeating branch cell units, and a corona or outer shell. The branch cells (BC), also known as *repeating units* (RU), are defined in terms of a branching angle,

Handbook of Polymer Synthesis, Characterization, and Processing, First Edition. Edited by Enrique Saldívar-Guerra and Eduardo Vivaldo-Lima.

TABLE 30.1 Dendritic Molecule Discoveries in the Literature

Year	Authors
Cascade Growth and Dendrimers	
1978	Vögtle [1]
1982	Maciejewski [3]
1983	de Gennes [4]
1985	Tomalia [5], Newkome [6]
1990	Hawker and Fréchet [7], Miller and Neenan [8]
Random Hyperbranched Polymers	
1988	Gunatillake et al. [9]
1990	Kim and Webster [10]
1991	Hawker et al. [11]
Dendrigraft Polymers	
1991	Gauthier and Möller [12], Tomalia et al. [13]

Source: Adapted with permission from Tomalia DA, Fréchet JMJ. J Polym Sci A Polym Chem 2002;40:2719 [2]. Copyright John Wiley and Sons.

rotation angles, RU lengths, and terminal groups. The covalent assembly of these BC can take place in a symmetrical manner, as in dendrimers, or into random irregular patterns for hyperbranched polymers. The size, shape, and functionality of the dendritic species depend on the synthetic strategy employed and can be different for each generation and/or each subclass of dendritic species.

The unique architecture of dendritic polymers affords distinct physical properties to these molecules as compared to their linear polymer analogues. For example, as shown in Figure 30.2, branched molecules have a much lower intrinsic viscosity than their linear analogues. Their compact and dense molecular configuration also leads to enhanced solubility at high molecular weights.

Some of the procedures used to synthesize dendritic molecules can be quite involved, and many different methods have been reported. The following three sections provide an overview of some of the pioneering work yielding each of the three main subclasses of dendritic polymers, namely, dendrimers, hyperbranched polymers, and dendrigraft polymers. The general characteristics and properties of these materials are also considered, as well as some of the more recent work including potential applications for these extremely versatile materials.

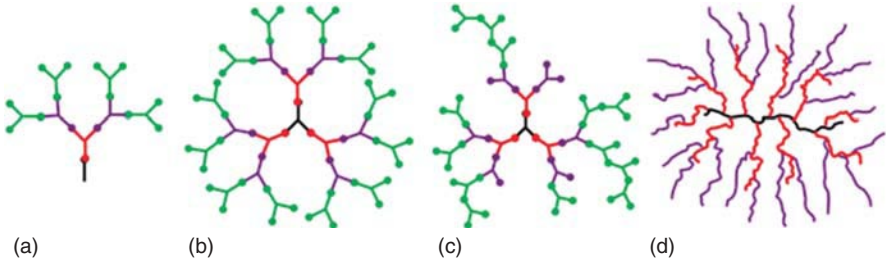

Figure 30.1 Structure of four types of dendritic polymers: (a) dendron, (b) dendrimer, (c) hyperbranched polymer, and (d) dendrigraft polymer. (*See insert for the color representation of the figure*.)

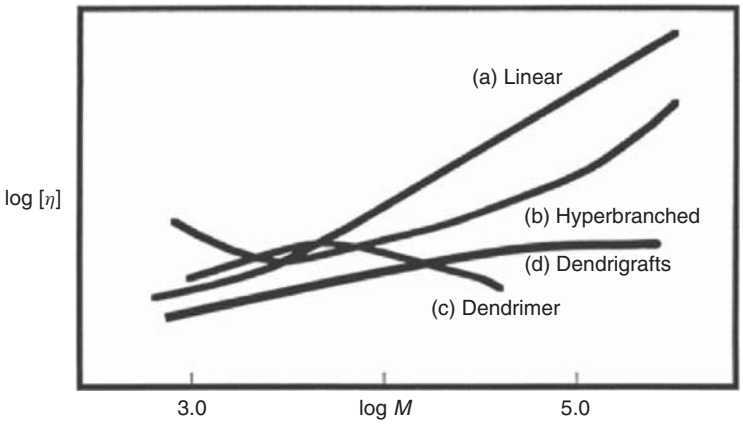

Figure 30.2 Molecular weight dependence of intrinsic viscosity $[\eta]$ for polymers with (a) linear, (b) hyperbranched, (c) dendrimer, and (d) dendrigraft architectures. *Source*: Reproduced with permission from Tomalia DA, Fréchet JMJ. Introduction to the dendritic state. In: Tomalia DA, Fréchet JMJ, editors. Dendrimers and Other Dendritic Polymers. West Sussex: Wiley; 2001. p 3 [14]. Copyright 2001 John Wiley and Sons.

30.2 DENDRIMERS

The word *dendrimer* is derived from the Greek words for tree- or branchlike (dendron) and part (meros). The strictly controlled structure of ideal dendrimers results from the layered assembly of BC surrounding the core, which is attained through sequential reaction cycles. This can be achieved in two different ways, namely, by divergent (core-first) or convergent (arm-first/core-last) methods.

30.2.1 Synthetic Strategies and Properties

The divergent approach begins with a multifunctional core onto which polyfunctional monomers of the AB_n-type are added. Dendrimers result when the branching multiplicity (subscript n) of the monomer unit is at least 2. Following the addition of these small-molecule building blocks, the subsequent layer can be added after deprotection of the end groups and another monomer condensation reaction. The structure resulting after the first addition cycle is known as a *generation 1 (G1) dendrimer*. Further reaction cycles are employed to prepare dendrimers of the desired generation, size, or molecular weight.

The convergent approach uses monomers similar to the divergent strategy and provides branched molecules with the same characteristics and predictability; however, wedgelike dendrons are first synthesized and subsequently anchored on a core to complete the dendritic structure. The number of dendrons that can be coupled with a core is governed by the core functionality. Convergent growth of the dendron occurs through selective protection of one of the functional groups, followed by a condensation reaction, resulting in directional growth. The dendron unit is interesting in itself, and it has been investigated as its own entity, but deprotection and coupling with a multifunctional "anchor" core is required to complete the dendrimer structure.

A comparison of the divergent and convergent strategies for the synthesis of a generation 2 (G2) dendrimer is provided in Scheme 30.1, where functionality A selectively reacts with functionality B, and P represents a protecting group for the associated functional group.

The divergent synthesis (Scheme 30.1a) begins with an unprotected trifunctional initiating core ($N_c = 3$). The G0 core can be coupled with a partially protected monomer, $BA_2(P)_2$, having a branching multiplicity (N_b) of 2. The G1 dendrimer results after removal of the protecting group on the A functionality ($-P_A$). Coupling of this substrate with the protected monomer yields what is referred to as a *half-generation dendrimer* (G1.5), and the G2 dendrimer is obtained on deprotection. The convergent synthesis starts by coupling a partially protected monomer, $B(P)A_2$, with a complementary protected monomer, $BA_2(P)_2$, to yield a dendron. Deprotection of the B group ($-P_B$) at the focal point of the dendron allows selective coupling with the G0 core (A_3) to obtain the G1.5 dendrimer. Deprotection of the terminal A functionalities provides the G2 dendrimer. Specific details on the chemistry for the functionalization, condensation, and protection processes are discussed subsequently.

The radial core-to-surface direction of the synthesis for the divergent strategy and surface-to-core direction for the convergent method should yield identical architectures, albeit some differences in properties have been observed for molecules obtained by both methods and deemed to have identical compositions. This can be explained in terms of the degree of structural perfection attained in each case. The divergent strategy requires the reaction of an exponentially increasing number of functional groups over successive generations. Considering the large number of reactions required for the complete conversion of all terminal groups, the probability of attaining a perfect structure is reduced.

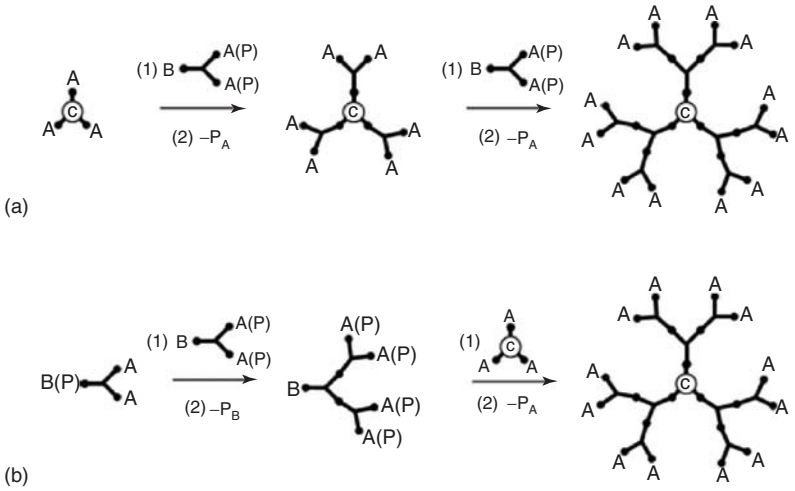

Scheme 30.1 Synthesis of a G2 dendrimer by (a) divergent and (b) convergent strategies.

This contrasts with the small number of coupling reactions involved in each cycle of a convergent synthesis. A lower degree of surface congestion also exists for the synthesis of individual dendrons, which favors complete reactions.

While the convergent strategy facilitates monomer coupling for upper generations independently of surface packing, the coupling of large dendrons to the anchor core is also more difficult due to steric hindrance making the focal point less accessible. Reduced coupling efficiency of the dendrons with the core has a more profound effect on the homogeneity of the dendritic species generated as compared to a reduced coupling efficiency for small-molecule monomers on the periphery of dendrimer in a divergent approach. The extent of surface congestion by terminal dendrimer groups can be estimated from the ratio of the dendrimer surface area (A_D) to the number of surface groups (Z) according to Equation 30.1, corresponding the surface area occupied per end group (A_z):

$$A_z = \frac{A_D}{Z} = \frac{4\pi r^2}{N_c N_b^G} \tag{30.1}$$

The generation at which the area available per end group approaches the actual dimensions of the end group is the point where incomplete reactions should become significant, resulting in an imperfect structure. This dense or critical packing state was predicted by de Gennes for polyamidoamine (PAMAM) dendrimers [4]. It was thus predicted that the onset of deviation in molecular weight from the ideal structure would occur around generation 9 or 10 for dendrimers, while molecular weight deviations were experimentally observed for generations as low as 4, but these nonetheless became more predominant from generations 9 or 10 as expected. Surface crowding effects and surface functionalization can play important roles in the application of dendrimers as scaffolds or containers: for example, a densely packed surface may inhibit loading of the dendrimer and rather favor surface coordination. Conversely, the flexible and more open structure of lower generation dendrimers should enhance their ability to house materials within their interior.

30.2.2 General Characteristics

The size, shape, and molecular weight of a dendrimer depend on the molecular weight and the branching multiplicity of the monomer, as well as its generation number. Molecular weights can range from the hundreds or thousands for low generations, to over 10^5 for generations 10 and above. The corresponding diameter of these structures ranges from circa 1 to above 10 nm. Different generations of dendrimers derived from a trifunctional core are compared in Scheme 30.2.

The three-dimensional topology of dendrimers displays a transition from ellipsoidal to spherical for increasing generations [16]. The onset of the morphogenesis is reliant on the core multiplicity and the synthetic strategy (divergent or convergent) used. Increased core multiplicity ($N_c = 3$ or 4 vs $N_c = 2$) forces a shape change at least one generation earlier. The convergent method has a similar effect due to the more perfect structure (increased crowding) attained for a particular generation. The most significant transformations occur between generations 3 and 5, after which the dendritic species adopt either spheroidal or slightly ellipsoidal geometries. An increase in generation number also brings enhanced surface group congestion, until a maximum known as the *dense packing state* is reached. Beyond this point, only a fraction of the end groups can participate in the next cycle of monomer addition.

Targeting a specific molecular weight and number of functional groups in dendrimer synthesis is relatively easy due to the uniform structure of the molecules, in as much as complete reactions are possible. The molecular weight (MW) and the number of terminal functional groups (Z) of dendrimers are well-defined functions of the core multiplicity (branching functionality N_c), the branch cell multiplicity (N_b), and the generation number (G) of the molecules. The number of functional groups can be calculated according to the following equation:

$$Z = N_c N_b^G \tag{30.2}$$

The number of end groups is directly related to the number of covalent bonds formed in each reaction cycle,

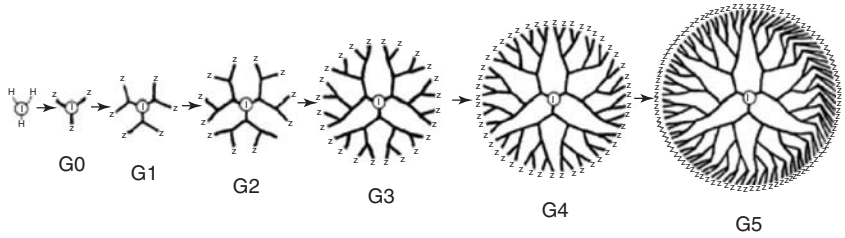

Scheme 30.2 Dendrimer generations derived from a trifunctional core and a monomer with a branching multiplicity of 2. *Source*: Reproduced with permission from Tomalia DA, Berry V, Hall M, Hedstrand DM. Macromolecules 1987;20:1164 [15]. Copyright 1987 American Chemical Society.

which increases according to the power law. The total number of BC in the structure can be calculated from Equation 30.3. The total number of BC is analogous to the degree of polymerization (DP) commonly cited for linear polymers and is also equivalent to the number of covalent bonds formed in the dendrimer:

$$\mathrm{BC} = N_\mathrm{c}\left[\frac{N_\mathrm{b}^G - 1}{N_\mathrm{b} - 1}\right] \tag{30.3}$$

The overall molecular weight of the dendrimer can be calculated by factoring in the molar mass of the various components including the core (M_c), repeat units (M_RU), and terminal groups (M_Z), as expressed in the following equation:

$$\mathrm{MW} = M_\mathrm{c} + N_\mathrm{c}\left[M_\mathrm{RU}\left(\frac{N_\mathrm{b}^G - 1}{N_\mathrm{b} - 1}\right) + M_Z N_\mathrm{b}^G\right] \tag{30.4}$$

30.2.3 Common Structures

30.2.3.1 Dendrimers Synthesized by a Divergent Strategy The concept of branched macromolecules derived from repetitive reaction cycles of multifunctional small molecules was first introduced in 1978 [1]. Vögtle thus reported a cascade-type divergent synthesis for low molecular weight polypropylenimine by the cyanoethylation of various amines cited in Reference 1, using acrylonitrile in glacial acetic acid at reflux for 24 h. Subsequent reduction of the cyano functionalities with cobalt(II) chloride hexahydrate and $NaBH_4$ in methanol converted the terminal cyanoethyl groups to primary propylamine functionalities, which were subjected to further cyanoethylation and reduction reactions to obtain the upper generation cascade polymers.

The yield of the cyanoethylation and reduction reactions in Vögtle's work was less than ideal, varying from 76% for the zeroth generation to 35% for the G1 product. These low yields resulted in ill-defined structures and prevented the synthesis of the upper generation structures. This procedure was nevertheless improved upon in the early 1990s after optimizing the cyanoethylation and hydrogenation reactions, by working in aqueous solutions at 80 °C and through hydrogenation with Raney cobalt, respectively [17, 18]. In this case, diaminobutane (DAB) served as multifunctional core to generate DAB-*dendr*-$(CN)_x$ and DAB-*dendr*-$(NH_2)_x$ dendrimers after the cyanoethylation and hydrogenation reactions, respectively. The reaction sequence for the divergent synthesis of polypropylenimine dendrimers is shown in Scheme 30.3.

PAMAM dendrimers, synthesized subsequently, are likely the most widely investigated and used dendritic polymers to date. The first dendrimers commercialized in that family were the Starburst® systems. These species were developed in the mid-1980s by Tomalia [5], at about the same time when Newkome developed similar dendritic architectures named *Arborols* [6]. A major incentive for the development of these molecules was the creation of covalently bonded (unimolecular) micelles comparable to the well-known multi- or intermolecular micellar systems.

PAMAM dendrimers are versatile in that their terminal groups can be easily modified for targeted functionality or reactivity. These compounds are synthesized by the condensation of amines and acrylates. An initiating core containing one or more amine functionalities is first reacted with an excess of methyl acrylate, resulting in an alkyl ester branch addition at each amino hydrogen (Scheme 30.4). This ester-terminated product is referred to as the *G0.5 dendrimer*. Amidation of the ester with ethylenediamine (EDA) causes branch extension with terminal amino groups. This amine-terminated dendrimer is referred to as a *G1 PAMAM dendrimer*. Repetitive cycles of Michael addition of the acrylate ester and amidation with EDA leads to successive generations of dendrimers. Functional group modification chemistry can also be performed on the terminal ester or amine groups. Thus, the treatment of the half-generation (ester-terminated) PAMAM dendrimers with alkali metal hydroxides yields carboxylate functionalities.

30.2.3.2 Dendrimers Synthesized by a Convergent Strategy Hawker and Fréchet [7] made a major contribution to the dendritic polymer chemistry field by developing a convergent approach to dendrimer synthesis in 1990. Dendritic fragments (dendrons) of benzyl ether were thus created by coupling phenols with benzylic halides. This approach represents a surface-to-core method, where the monomers are assembled from the peripheral units toward the core. Benzyl bromide was first coupled with dihydroxybenzyl alcohol (DHBA) in the presence of potassium carbonate and 18-crown-6 as a phase transfer catalyst in acetone as shown in Scheme 30.5. Following isolation and purification of the product, the

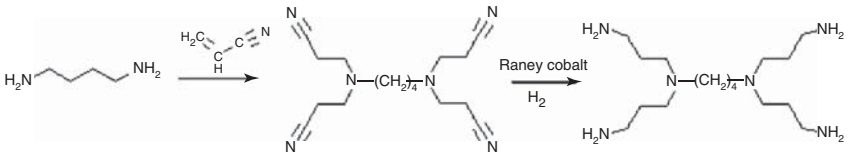

Scheme 30.3 Preparation of polypropylenimine dendrimers.

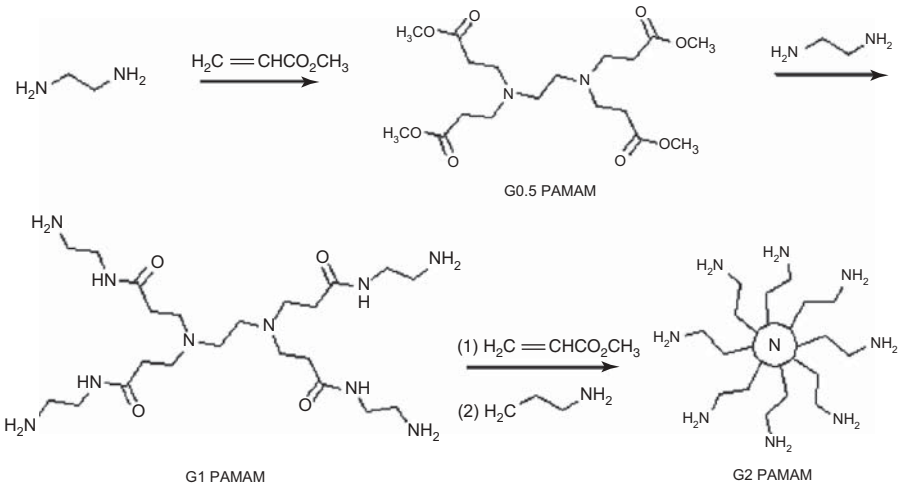

Scheme 30.4 Divergent PAMAM dendrimer synthesis starting from a diamine (EDA) core.

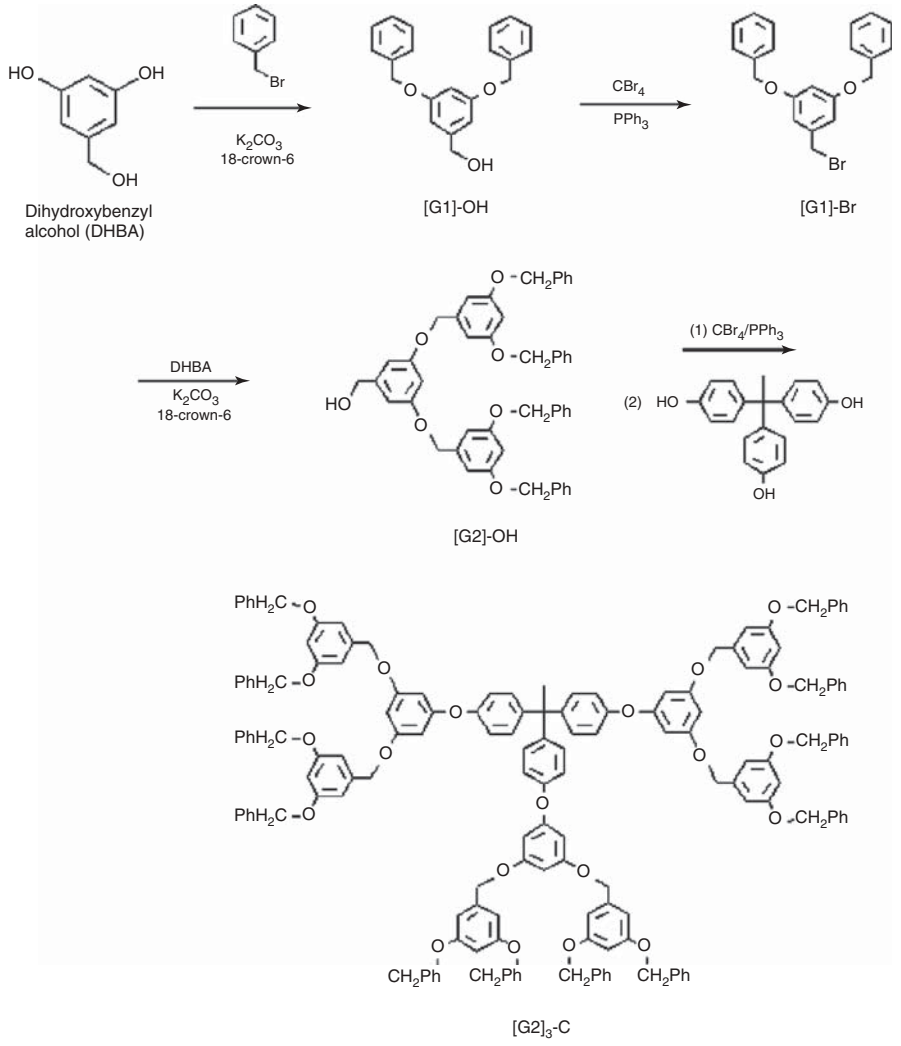

Scheme 30.5 Synthesis of a Fréchet-type benzyl ether dendrimer by a convergent approach.

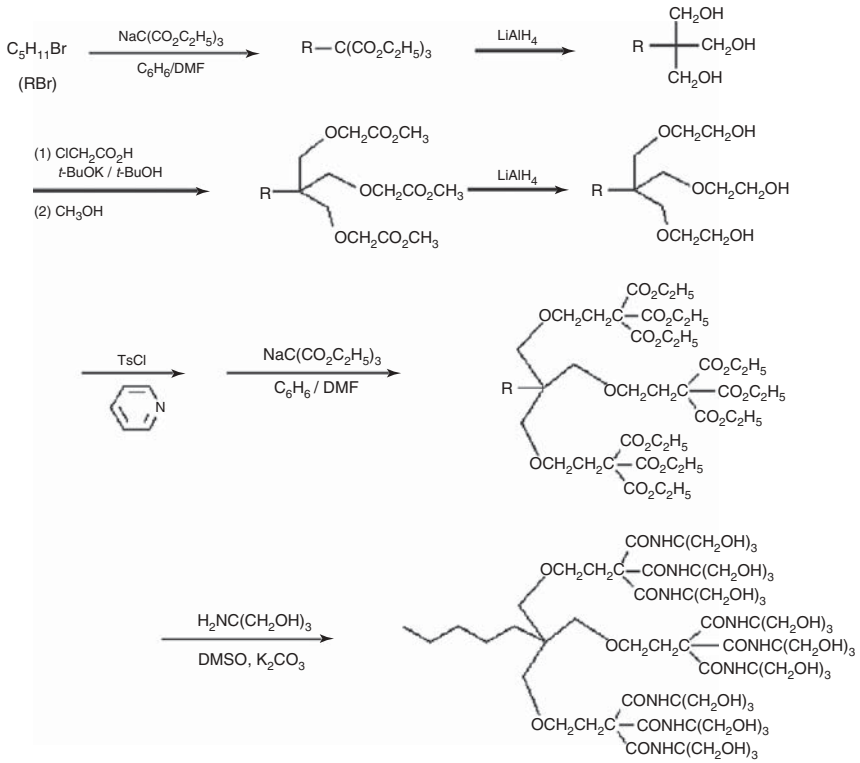

Scheme 30.6 Arborol synthesis according to Newkome.

G1 dendritic benzyl alcohol was converted to a benzylic bromide by treatment with carbon tetrabromide and triphenylphosphine. Further cycles of DHBA monomer coupling were performed to obtain subsequent dendron generations. To obtain a symmetrical dendrimer, the dendritic wedges carrying a bromide functionality at their focal point can be coupled with a polyfunctional core such as 1,1,1-tris(4′-hydroxypheny1)ethane.

A convergent strategy such as this, with only one final coupling step for the dendron wedges, facilitates high yield reactions leading to well-defined structures. The symmetry of the molecules can be controlled through the functionality of the anchoring core.

In fact Newkome was really the first one to report a convergent dendron synthesis for the preparation of arborols, but the generation number and the molecular weight attained were limited [6]. The synthesis of arborols started from a trifunctional branch cell formed by treating an alkyl halide with triethyl sodium methanetricarboxylate. Subsequent reduction of the ester with $LiAlH_4$ yielded a triol. The formation of the second tier through another cycle of esterification was attempted by tosylation with tosyl chloride in pyridine and treatment with the methylsodium triester, but the yield was very low due to inefficient nucleophilic attack at the three terminal sites as a result of steric crowding. To solve this issue, extension of the ester was performed before tosylation and coupling with the methylsodium triester to afford the nonaester. The third generation of this cascade molecule, obtained through amide functionalization with tris(hydroxymethyl)aminomethane, was completely water soluble. The reaction scheme for Newkome's synthesis of a 27-arm arborol is shown in Scheme 30.6.

30.2.4 Applications and Recent Trends

Considering the extensive control achieved over the size, shape, and surface functionality of dendrimers, it is not surprising that these molecules have a wide range of potential applications. On examination of the structural features of a dendrimer, one can visualize sector-specific uses as shown in Figure 30.3.

The first application examined, and one of the primary motivations for dendrimer syntheses, was as unimolecular micelles. In contrast to common micellar structures formed through intermolecular association or aggregation, dendrimers are covalently bonded structures unaffected by their surrounding environment. Consequently, the ability of amphiphilic dendrimers to encapsulate guest compounds should be independent of changes in concentration, solvent, and pH, among others. A strong incentive for dendrimer micelles is in catalysis. Considering the structure and functionality control attained, catalytic sites can be introduced specifically within the core, on the periphery of dendrimers, or both, as illustrated in Figure 30.4.

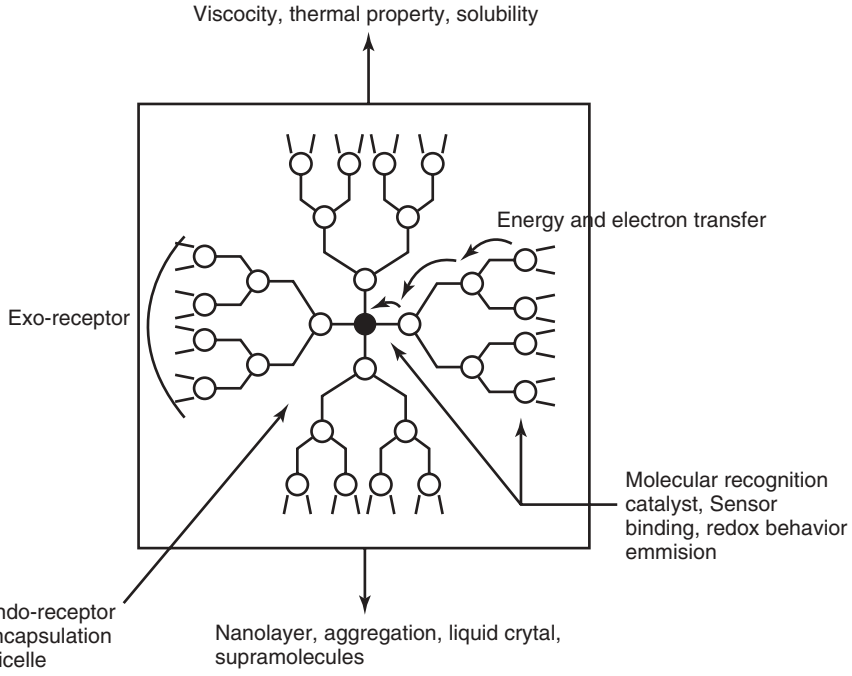

Figure 30.3 Structural features and potential uses of dendrimers. *Source*: Reproduced with permission from Inoue K. Prog Polym Sci 2000;25:453 [19]. Copyright 2000 Elsevier.

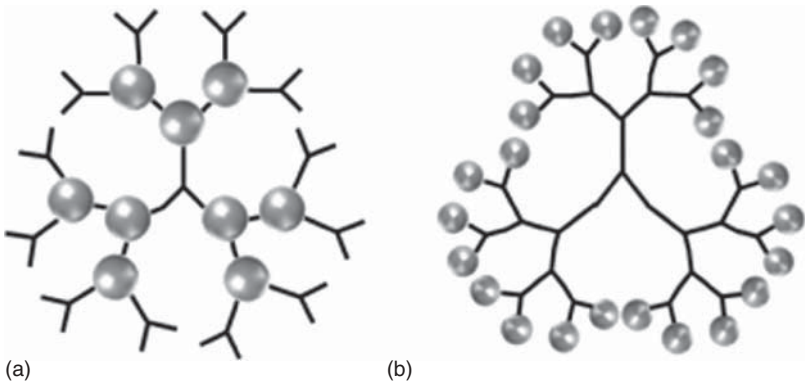

Figure 30.4 (a) Internal and (b) peripheral dendrimer functionalization.

The preparation of metallodendrimers, incorporating metallic species within their structure, is a relatively facile process given the ease and versatility of dendrimer functionalization which can be tailored for metal coordination. For example, the PAMAM dendrimers discussed earlier can coordinate different transition metals through their nitrogen atoms. Metals able to coordinate with the PAMAM structure include among others Cu [20, 21], Au [22], Pd [23], Pt [24], Ag [25], Co [26], as well as bimetallic systems such as Pd–Au [27] and Pt–Ru [28]. Dendritic catalyst selectivity, activity, and stability can vary on the basis of steric effects, the location of the catalyst, and the architecture of the dendritic support [29, 30].

Coronal functionalization of the dendrimers with metals is typically performed by a divergent approach, that is, with the metal binding process occurring in the final step. Catalysis on the periphery of dendrimers provides easily accessible sites; however, steric crowding of the reactants can influence the activity level observed. In theory, such a system should have a performance comparable to homogeneous (nonsupported) systems [31]. A higher loading level (catalyst/dendrimer) is possible with peripheral loading, as there is a larger number of terminal groups as compared to junctions within the dendrimer skeleton; however, core-functionalized metallodendrimers offer isolated catalytic sites that can be attractive for

certain applications. In many cases, the reduction of the noble metal salts is necessary after loading into the dendrimer. Alternately, the reduction of surface-bound metals could result in encasement of the dendritic structure, and potentially eliminate some of the inherent benefits that the core may have, or create a barrier to core loading. Careful selection of the surface functionality and the degree of functionality are critical. In both core- and periphery-functionalized metallodendrimers, isolation of the catalyst from the crude product is conveniently achieved by nanofiltration. Several reviews have been published on this topic [31, 32].

Examples of peripherally functionalized catalysts include carbosilane dendrimers with Ni at their peripheral functional sites serving in the Kharasch addition of polyhalogenoalkanes to terminal carbon–carbon double bonds, which displayed regioselectivity [33]. Polypropylenimine dendrimers have likewise been end-functionalized with palladium, rhodium, iridium, and Pd–Ni bimetallic catalysts for use in the Heck reaction and hydroformylation [34]. PAMAM dendrimers supported on silica were complexed with rhodium for heterogeneous catalysis in the hydroformylation of styrene and various other olefins. The highly active catalyst yielded branched chain aldehydes with high selectivity from aryl olefins and vinyl esters. The catalyst was easily recovered, and no significant loss in selectivity or activity was observed on reuse [35].

Core-functionalized metallodendrimer catalysts are sometimes referred to as *dendrizymes* by analogy to biological systems and due to the observed influence of the generation number on selectivity. Ferrocenyldiphosphine core-functionalized carbosilane dendrimers have thus been prepared as Pd ligands for the homogeneous catalysis of allylic alkylation reactions, and displayed variations in product selectivity for the largest dendrimers investigated [36]. Fréchet-type polyether dendrons were complexed with Pt for use as SO_2 sensor and with Ni for the Kharasch addition of CCl_4 to methyl methacrylate [37]. The dendron wedges, when functionalized at their focal point, displayed adequate catalytic activity with easy recovery and good stability.

Mimicking biological species is a major investigation area for dendrimers, particularly for PAMAM-based structures due to their similarities in size, shape, and chemical make-up with globular proteins. Thus, the immunodiagnostic capabilities of dendrimers have been investigated [38], as well as *in vitro* and *in vivo* gene delivery [39] and gene expression [40]. These species possess an exterior barrier controlled through end-group functionalization, as well as void spaces within their interior, much like liposomes. The tailored unimolecular micelle characteristics of dendrimers, with an open interior (in contrast to typical micelles), allows them to entrap guest molecules of various sizes and to selectively release them under certain conditions [41]. These characteristics have led to the development of macromolecular drug delivery systems from dendrimers. In analogy to other complexation processes, drug molecules can be loaded inside or attached at the periphery of the molecules, to form dendrimer–drug conjugates. In the latter category, it has been demonstrated that PAMAM dendrimer–platinate conjugates have antitumor activity [42]. More recently, it was shown that the encapsulation or complexation of camptothecin (a plant alkaloid known for its anticancer potency) with PAMAM dendrimers increased its solubility, which represents a step toward the effective delivery of this drug to cancerous cells [43]. PAMAM dendrimer–glucosamine conjugates have even been shown to prevent scar tissue formation [44]. Lastly, dendrimers have been investigated for light-harvesting applications [45]. Their branched architecture provides an interesting framework in which energy transfer can occur from peripheral chromophores to an energy sink located at the core of the molecules. This property can be exploited in light-emitting diodes, frequency converters, fluorescent sensors, or as a mimic for the natural photosynthesis process.

30.3 HYPERBRANCHED POLYMERS

Hyperbranched polymers also possess a dendritic architecture, but with imperfect branching. The basic structural features present in these molecules are the same as in dendrimers, namely, a core surrounded by layers of BC capped with terminal units. The one-pot syntheses used to create these treelike structures also rely upon AB_n-type monomers (Scheme 30.1), but without protecting groups preventing simultaneous condensation reactions. The resulting polymers typically have broad MWD ($Đ > 2$), with multiple isomers and geometries. Because they are created in a single reaction step, hyperbranched polymers are more economical to produce than dendrimers as their synthesis is less time and resource intensive. This trait represents a major draw for industry and the development of commercial applications for dendritic polymers

30.3.1 General Features

Many methods have been reported to synthesize hyperbranched polymers. These materials were first reported in the late 1980s and early 1990s by Odian and Tomalia [9], Kim and Webster [10], and Hawker and Fréchet [11]. As early as 1952, Flory actually developed a model for the polymerization of AB_n-type monomers and the branched structures that would result, identified as random AB_n polycondensates [46]. Condensation step-growth polymerization is likely the most commonly used approach; however, it is not the only method reported for the synthesis of statistically branched dendritic polymers: chain growth and ring-opening polymerization methods have also been applied,

among others. In a one-pot (or concurrent) method, the monomers simply add in alternate manners into patterns that can be modeled statistically. Structures can be grown in the presence or the absence of a central core, as illustrated in Scheme 30.7 for a simplified system.

Ideally no intermolecular reactions should occur between the branched structures, but this is difficult to avoid in many cases and is a drawback to this method. For such an ideal (and simplified) case with an AB_2-type monomer, the branching coefficient (α), representing the probability that a branch unit has reacted, and is thus connected to another branch unit, is equal to the fraction of B groups reacted (p_B), if it is assumed that the two B moieties are equally reactive. The probability or fraction of A groups having reacted (p_A) can then be considered to represent the extent of reaction, which leads to the relation between the extent of reaction (p), the branching coefficient (α), and the functionality of the AB_x monomer (f) given by the following equation [46]:

$$\alpha = p_B \text{ and } p_A = p_b\,(f-1)\,\text{; therefore,}$$
$$\alpha = \frac{p_A}{f-1} = \frac{p}{f-1} \tag{30.5}$$

Fréchet proposed to use the ratio of the number of fully branched monomer units to the total number of monomer units contained within the polymer (N_o) to describe the degree of structural perfection of hyperbranched polymers derived from AB_2-type monomers [11]. In a dendrimer with a perfect structure, two types of monomer units are present in equal proportions, the terminal (T) and the dendritic (D) units, and thus the degree of branching is equal to 1. In a hyperbranched structure, some of the dendritic units are unreacted, leading to the formation of a third monomer unit described as a linear (L) segment. The degree of branching (α_{Fr}) attained under these conditions can be expressed by Equation 30.6, where D, T, and L represent the total number of each type of unit:

$$\alpha_{Fr} = \frac{D+T}{D+T+L} = \frac{D+T}{N_o} \tag{30.6}$$

The different types of dendritic monomer units are shown in Figure 30.5, where the dendrimer (Fig. 30.5a) contains three dendritic and six terminal groups, while the hyperbranched structure (Fig. 30.5b) has two dendritic, three linear, and five terminal units, yielding branching functionalities (as defined by Fréchet [11]) of 1 and 0.7, respectively.

The relative amounts of each of the three types of monomer units can, in some cases, be determined by NMR analysis or by other spectroscopic methods. In situations where the units cannot be differentiated by these methods, selective labeling and/or degradation can be performed, followed by spectroscopic analysis. It should be noted that Equation 30.6 does not tend toward zero for linear polymers as it should. This discrepancy prompted the development

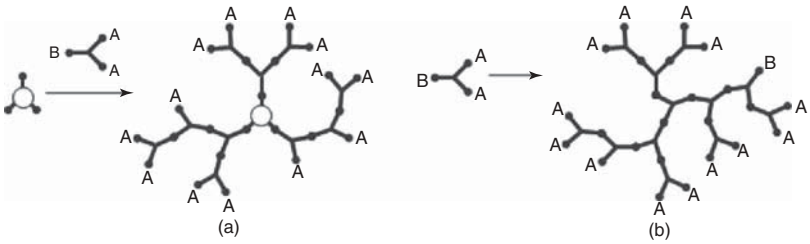

Scheme 30.7 (a) Core and (b) noncore methods for the synthesis of hyperbranched polymers.

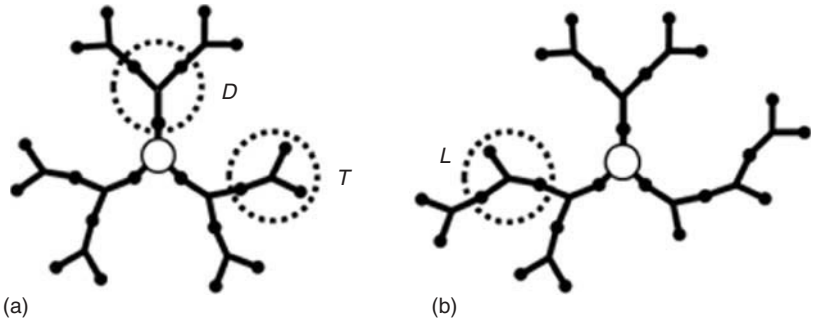

Figure 30.5 Structural units in a dendrimer (a, $\alpha_{Fr} = 1$) and a hyperbranched polymer (b, $\alpha_{Fr} = 0.7$): dendritic (D), linear (L), and terminal (T).

of a corrected expression for branching functionality (α', Eq. 30.7) by two different groups in 1997 [47, 48]. Expressions for the universal degree of branching were also derived for higher order functionalities and can be found in the respective references:

$$\alpha' = \frac{2D}{2D + L} \tag{30.7}$$

In his original 1952 article [46], Flory also predicted the influence of branching on the DP and molecular weight dispersity, as shown in the following equation, which is derived from Equation 30.5:

$$Đ = \frac{X_w}{X_n} = \frac{1 - \alpha^2 (f - 1)}{1 - \alpha (f - 1)} \tag{30.8}$$

It is apparent that the breadth of the MWD is highly dependent on the extent of reaction (conversion) attained in these reactions, as $Đ$ increases with the conversion. At low conversions, the MWD for an AB_n system corresponds to a Flory distribution ($Đ \approx 2$); however, $Đ$ trends toward infinity as full conversion is approached. For trifunctional monomers, including equally reactive A_3 monomers and ABC monomers with reactivity differentials, the MWD also depends on the DP but in a different way: $Đ$ is proportional to DP in an A_3 system, while for an ABC system it is proportional to $(DP)^{1/2}$ [49, 50].

Unfortunately, the one-pot reaction scheme for the preparation of hyperbranched polymers offers no option for molecular weight control, which ultimately leads to gelation. Intramolecular side reactions such as cyclization resulting from "backbiting" processes are also common in these reactions. One technique developed to avoid or reduce side reactions uses a slow monomer addition protocol, by adding monomer throughout the reaction. This method has been termed *concurrent slow addition* [51–53]. The copolymerization of AB monomers with AB_2 monomers has also been employed to control the molecular weight and reduce $Đ$ in these reactions [51, 54]. Multifunctional initiators (B_y monomers), when used in batchwise or concurrent slow addition protocols, have also shown promise in controlling the breadth of the MWD [55, 56].

30.3.2 Synthetic Strategies and Common Structures

Hyperbranched polymers can be synthesized by either single- or double-monomer methods. Falling in the single-monomer methodology (SMM) are common polymerization techniques including the polycondensation of AB_n monomers, self-condensing vinyl polymerization (SCVP), self-condensing ring-opening polymerization (SCROP), and proton-transfer polymerization (PTP). The double-monomer methodology (DMM), as the name suggests, relies on monomer pairs that can be subdivided into two strategies: $A_2 + B_3$ reactions, and the couple-monomer methodology (CMM). Many combinations of compatible monomers have been successfully applied to these strategies. Considering the broad scope of this topic, only a few examples of the pioneering work and some of the simpler methods are provided for the different strategies. A more detailed review on synthetic strategies for the preparation of hyperbranched polymers was provided by Gao and Yan [57].

30.3.2.1 Single-Monomer Methodology Kim and Webster reported the first example of a single-monomer polycondensation technique using 3,5-dibromophenylboronic acid and aqueous sodium carbonate in the presence of a Pd catalyst [10]. A general scheme corresponding to this reaction and the resulting hyperbranched structure obtained are shown in Scheme 30.8.

The single-monomer polycondensation scheme has also been used to synthesize hyperbranched polyethers [58], polyesters [59], polyurethanes [60], polysiloxysilanes [61], as well as polycarbonates [62]. Higher order monomers including AB_3, AB_4, AB_5, and AB_6 have also been applied in single-monomer polycondensation syntheses of hyperbranched polymers [63, 64].

SCVP requires a monomer not only with a vinyl group but also with a pendant moiety that can act as an initiating site for other vinyl pendants. This type of monomer is referred to as an *inimer* (initiator + monomer). Fréchet developed both free radical [65] and cationic [66] SCVP methods for the synthesis of hyperbranched molecules using inimers. These techniques all depend upon the same principle: new initiating species are formed from a specific functionality within the inimer molecules. Once activated, this site can propagate through vinyl groups on other monomers or inimers. As propagation continues, macromonomers formed from inimers in the reaction eventually react with the propagating center, resulting in branching.

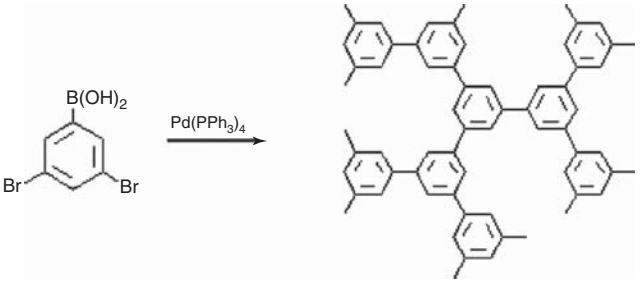

Scheme 30.8 Hyperbranched polyphenylene synthesis by the single-monomer polycondensation method.

In Fréchet's cationic method, 3-(1-chloroethyl)-ethenylbenzene is activated with $SnCl_4$ to yield a cationic initiating site from the chloroethyl functionality. This site can propagate through vinyl-containing species, producing chains with pendant initiating sites that form branches once they become active and participate in chain propagation. Similar reaction sequences are involved in the radical systems, for example, with a styrenic inimer containing a benzylic nitroxide functionality [65]. In this case, the hyperbranching process begins with the thermolysis of the benzylic nitroxide, producing radical species that propagate through the pendant vinyl group of the styrene moieties. Residual nitroxides can also cleave along the polymer backbone to form radical sites and propagate branch growth. The cationic and radical hyperbranching processes are illustrated in Scheme 30.9a and b, respectively.

The degree of branching attained in SCVP reactions is governed by the reactivity difference between chain growth through the vinyl groups and step growth addition at the initiating site. In some cases, the degree of branching attained can be controlled by adjusting the reaction conditions used. The radical SCVP procedure requires additional considerations, however, since side reactions leading to gelation are more probable at longer reaction times.

Polymerization by the inimer technology has received much attention from Kennedy and Puskas, specifically for the synthesis of hyperbranched polyisobutylenes (PIB)s and copolymers thereof in a one-pot method [67]. While this convergent approach complicates the structural analysis of the branched polymers, fragmentation of the resulting polymer is possible in some cases to allow such analysis [68]. Branching ratios (BR) can be calculated directly from the molecular weight of the branched polymer as per Equation 30.9, to give an indication of the number of branches contained within the molecules, as the ratio of the measured M_n for the polymer obtained to the theoretical M_n $\left(M_n^{theo}\right)$.

$$BR = \frac{M_n}{M_n^{theo}} - 1 \tag{30.9}$$

The theoretical M_n is calculated by assuming that all the inimer molecules in the reaction act solely as monofunctional initiator and not as a branching agent. This quantity is calculated from the mass of monomer (m_m) and the moles of inimer (n_i) in the reaction as described by the following equation:

$$M_n^{theo} = \frac{m_m}{n_i} \tag{30.10}$$

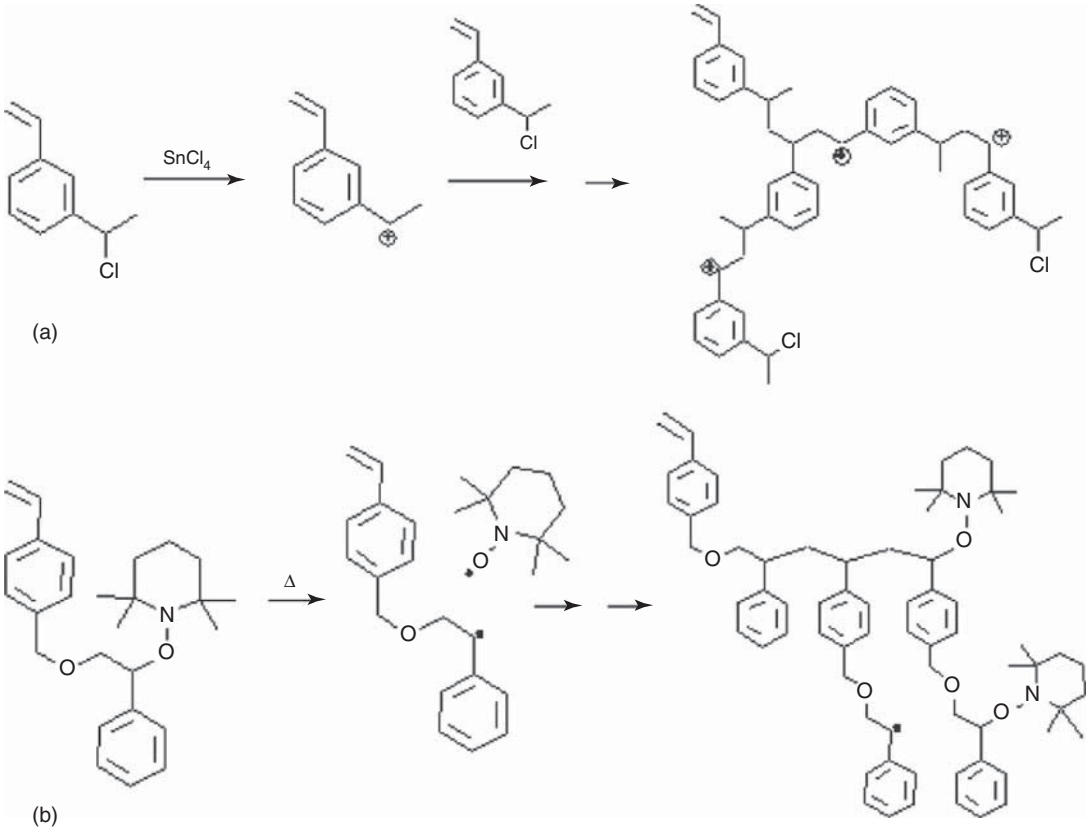

Scheme 30.9 Formation of hyperbranched polymers by (a) cationic and (b) radical SCVP.

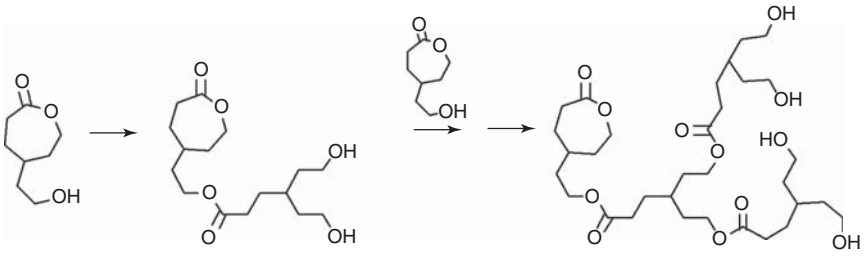

Scheme 30.10 SCROP of hydroxyl-functionalized caprolactone.

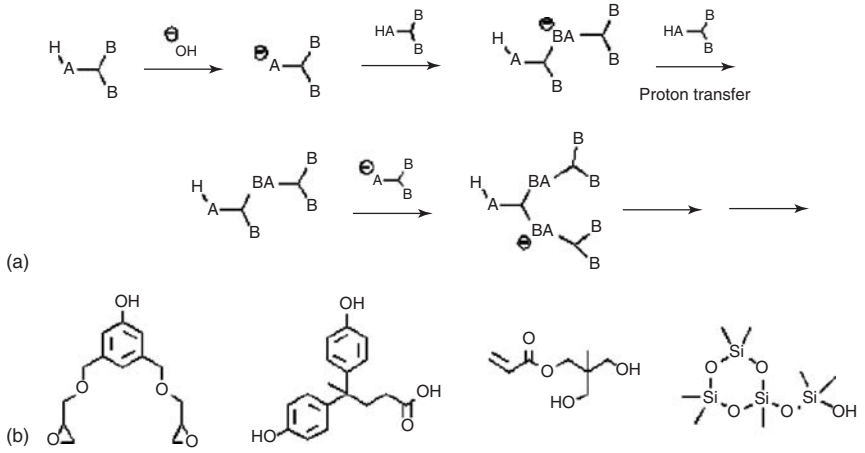

Scheme 30.11 (a) Generalized PTP synthetic scheme and (b) examples of monomers used in PTP syntheses.

SCROP and ring-opening multibranching polymerization (ROMBP) are similar to SCVP; however, in these cases, the inimer is a cyclic monomer carrying an initiating functionality. A good example of this approach is shown in Scheme 30.10, where hyperbranched polyesters are formed from inimers containing an alcohol functionality and a caprolactone group [69].

The dominant contribution of simultaneous chain growth from all the chain ends, controlled by the deprotonation level of the initiator, leads to relatively narrow MWD ($Đ \approx 1.1-1.4$) while maintaining branching levels typical of random polycondensation reactions (degree of branching $\alpha' \approx 0.5$, Eq. 30.7) [70]. The SCROP technique has also been used to synthesize hyperbranched polyglycerols [70], polyethers [71], and polyamines [72].

PTP, which began to gain momentum in the late 1990s, relies on a reaction sequence of the type shown in Scheme 30.11a, where a catalytic amount of initiator is added to the monomer for proton abstraction. Following coupling with another neutral monomer unit, a thermodynamically favorable proton-transfer reaction occurs from another free monomer unit to the dimer. The activated monomer can then couple with another monomer unit or with an existing branched species. The proton-transfer step does not propagate to a significant extent as it is a kinetically slower process. Specific monomers that have been investigated for the PTP method are shown in Scheme 30.11b.

30.3.2.2 Double-Monomer Methodology The most versatile approach to hyperbranched polymer synthesis is likely the double-monomer methodology (DMM), due to the wide range of monomers and chemical functionalities to which it can be applied. The two categories of DMM reactions only differ in terms of the reactivity of the functional groups involved: in $A_2 + B_3$ reactions, all the moieties within each monomer have the same reactivity, while varying degrees of reactivity describe the couple-monomer methodology (CMM).

The chemistry behind the $A_2 + B_3$ method is analogous to the previously described AB_n reactions, but the compatible reactive sites are separated on two different monomers. A significant obstacle in this approach is the occurrence of gelation, commonly observed for the direct polycondensation of A_2 and B_3 monomers. This problem can be minimized through slow monomer addition, capping agents, reaction quenching by precipitation, or the addition of catalysts or condensation agents before reaching the critical conversion point. A few of the less exotic monomer combinations that have been used in $A_2 + B_3$ reactions are depicted in Figure 30.6. These examples include monomers

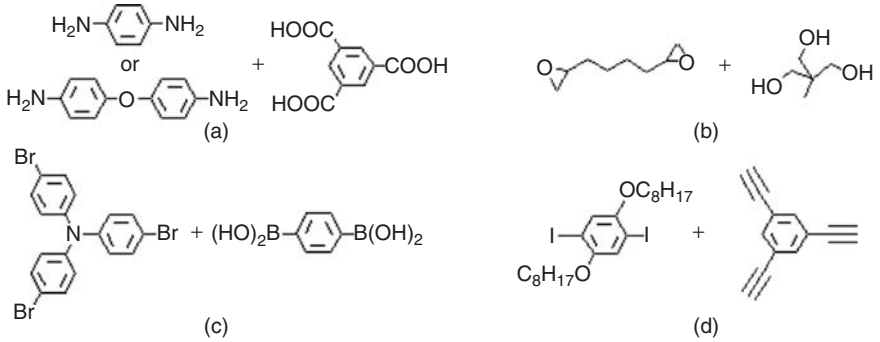

Figure 30.6 Examples of monomer combinations for the $A_2 + B_3$ double-monomer synthesis of hyperbranched polymers.

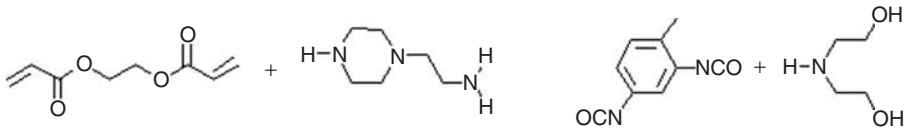

Figure 30.7 CMM monomers for (a) $A_2 + B' B_2$ and (b) $A_2 + CB_n$ reactions.

with the following chemical functionality combinations: aromatic diamine and triacid (Fig. 30.6a) [73], diepoxy and trihydroxy (Fig. 30.6b) [74], trisbromophenyl and diboronic acid, (Fig. 30.6c) [75], and diiodophenyl and triethynylphenyl (Fig. 30.6d) [76].

The CMM provides improved control over the branching process through reactivity tailoring, resulting in soluble (nongelled) hyperbranched polymers in most cases. Gelation can be avoided through careful monomer selection whereby the reactivity of the functional groups differs. Many different monomer combinations have been reported fulfilling this requirement, two of which are $A_2 + B' B_2$ and $A_2 + CB_n$ systems. In the first case, both A groups have the same chemistry and reactivity, and likewise for the B groups, however, B′ has the same chemical make-up as B but differs in reactivity. In the $A_2 + CB_n$ system, the A groups and B groups have equivalent reactivity, but C differs in chemical structure and reactivity. Examples of monomers corresponding to each of these CMM classes are provided in Figure 30.7.

The first example, Figure 30.7a, is an $A_2 + B' B_2$ system with two equally reactive vinyl groups (A_2) and three amine functionalities, where the tertiary amine is unreactive under the conditions used. The primary and secondary amines differ in terms of reactivity and are bi- and monofunctional, respectively (B_2B'). In the $A_2 + CB_n$ case, Figure 30.7b, the isocyanate groups are considered to be equally reactive based on the CMM naming conventions (A_2), as are the hydroxyl groups (B_2), the third functional group being a secondary amine (C). Higher order functionalities have also been investigated. A hyperbranched analog of the commercially available PAMAM dendrimers (HYPAM) has thus been synthesized by a one-pot method shown in Scheme 30.12 [77]. This approach can be described as an

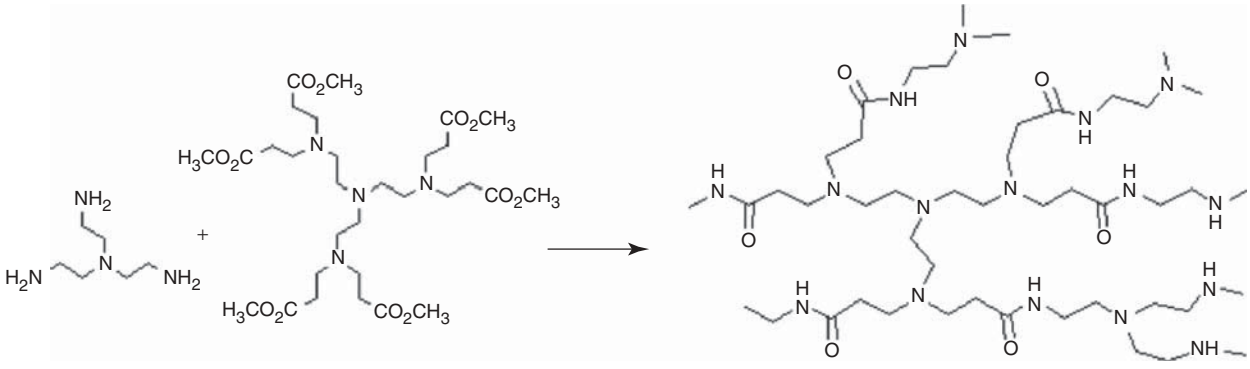

Scheme 30.12 Synthesis of hyperbranched PAMAM (HYPAM).

$A_6 + B_6$ reaction of tris(2-aminoethyl)amine with tris(2-di(methyl acrylate)aminoethyl)amine.

30.3.3 Applications and Recent Trends

The comparable architecture and chemical functionality of dendrimers and hyperbranched polymers lead to similar applications for these two families of dendritic polymers. The main benefit in using hyperbranched polymers to replace dendrimers lies in their simpler synthesis, provided that the perfect structure of dendrimers can be sacrificed for their broadly distributed hyperbranched analogs. The one-pot syntheses require less time and resources, resulting in less expensive processes that make hyperbranched polymers excellent candidates for commercial applications. Pertinent to the hyperbranched architecture are applications as electronic, magnetic, and catalytic materials, as well as numerous uses in the biomedical field; some of these are considered herein.

The incorporation of transition metals in hyperbranched polymers has received considerable attention. Like dendrimers, hyperbranched materials can be loaded with metals within their interior, on their exterior, or throughout the whole molecule, the exact location of the coordination sites depending on the functionality of the polymer, as shown previously in Figure 30.4. Salazar thus modified hyperbranched polyglycerol with hydroxyl end groups to a structure containing tertiary amines on its periphery [78]. The hyperbranched polyamines were coordinated with copper chloride and were successfully used as catalysts in the oxidative coupling reaction of phenylacetylene. Similarly, NCN-pincer platinum(II) carboxylates were complexed with hyperbranched polyglycerols to form endoreceptors to catalyze the coupling reaction of methyl vinyl ketone and ethyl α-isocyanopropionate by Michael addition [79, 80]. These systems displayed improved performance due to the enhanced accessibility of the catalytic sites and the high local reagent concentration; the catalysts could be isolated from the reaction product in high yield (>97%) by dialysis. Other mainstream hyperbranched polymers such as polyethylenimines [81] and PAMAMs [77] have also been used to stabilize various transition metals for catalytic applications. These molecules contain multiple metal-coordinating sites, both internal and peripheral, due to their high nitrogen content. The terminal primary amine groups of these polymers can also serve as functionalization sites to enhance the stability of the metal–polymer complexes under different solvency conditions. Thus, in the case of hyperbranched polyethylenimines, the aqueous solubility of the polymers loaded with transition metals (Cu, Ag, Au, and Pt) was ensured by encapsulating the structure with a carbohydrate shell [81].

The postpolymerization functionalization method to incorporate transition metals into hyperbranched polymer structures can target the interior cavities and the functional groups of the molecules alike. One of the more exotic applications proposed for a metal-loaded hyperbranched polymer is a combination of a semiconductor polymer of conjugated poly(*p*-phenylenevinylene) (PPV) and colloidal semiconducting CdS nanocrystals at various locations within the structure [82]. This was accomplished by incorporating alkoxy substituents within the monomer before the hyperbranched polymer synthesis, to provide coordinating sites for cadmium. The deposition of cadmium within the branched structure increased the dispersion of the nanoparticles and reduced their aggregation within the PPV-CdS hybrid, in addition to providing efficient energy transfer. The unique photochemical activity displayed by these nanostructured CdS materials make them excellent candidates for power conversion in hybrid photovoltaic systems [83]. Using a similar approach, a scaffold containing triple bonds acting as ligand sites was used to template the deposition of cobalt carbonyl, $Co_2(CO)_8$. The cobalt-containing hyperbranched polyynes were synthesized by Häußler et al. for the preparation of nanostructured magnetoceramics [84]. The cobalt was incorporated in the core of the hyperbranched polyynes through cobalt-triple bond coordination within the hyperbranched backbone. The structural units of the polymers used to template CdS and cobalt deposition are compared in Figure 30.8.

The incorporation of metals within dendritic structures during the synthesis of the molecules has been achieved using metal-containing AB_2 monomers. Onitsuka used this approach in the synthesis of hyperbranched polyyne from Pt-functionalized monomers [85]. These displayed liquid crystalline properties under the influence of a magnetic field, similar to the analogous one-dimensional linear structures [86]. The predetermined location of the metal within the monomer ensures its even and regular distribution throughout the entire polymer structure. An analogous Pt-containing dendrimer structure has also been reported [87]. The formation of a hyperbranched structure from the platinum–acetylide monomer proceeds as shown in Scheme 30.13.

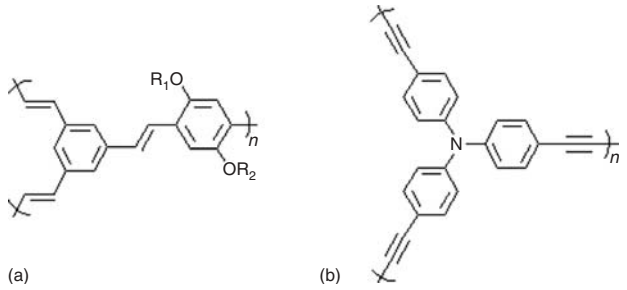

Figure 30.8 Conjugated hyperbranched polymers used to template (a) CdS and (b) cobalt deposition.

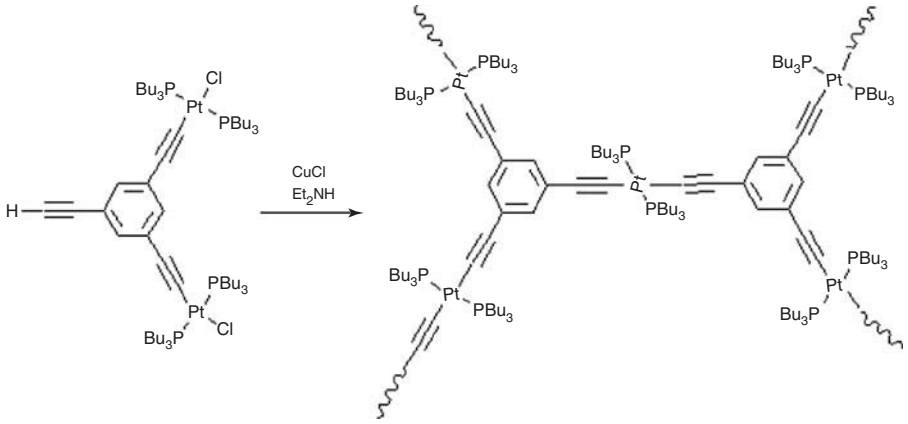

Scheme 30.13 Synthesis of a hyperbranched polymer from a platinum-containing acetylide monomer.

Hyperbranched polymers are also gaining interest as biomaterials, specifically as hosts for bioactive molecules such as drugs, labels, or probes. Hyperbranched polyglycerols are one of the candidates considered for this application as their synthesis is well-established and controlled, but more importantly they are biocompatible and biodegradable. End-group functionalization is also a versatile method that can be easily adapted for enhanced biocompatibility, for site targeting, or to serve as binding sites for guest molecules [88]. Similar polymers have been applied to protein immobilization [89, 90] or to support cell growth [91]. Hyperbranched PIB-based copolymers have likewise received significant attention as biomaterials, with specific interest as coatings in arterial stents [92, 93]. This is due to the fact that a linear triblock copolymer analog, poly(styrene-*b*-isobutylene-*b*-styrene) (SIBS), has received approval from the United States Food and Drug Administration (FDA) for use as medical device coating. More specifically, copolymers of PIB and styrenic monomers were shown to display thermoplastic elastomeric (TPE) properties and are being assessed for their degree of biocompatibility [94, 95]. The TPE properties of these materials arise from microphase separation of the polystyrene (PS) chain segments within the polymer matrix providing physical cross-links, in analogy to the common block copolymer TPE. Consequently, these materials behave like covalently crosslinked (vulcanized) rubbers at room temperature, but they can be processed like thermoplastics at temperatures above the glass transition temperature of the PS segments.

30.4 DENDRIGRAFT POLYMERS

30.4.1 General Characteristics

These macromolecules have a dendritic architecture reminiscent of dendrimers and hyperbranched polymers, but are derived from polymeric building blocks rather than small-molecule monomers. While the molecular weights attained for dendrigraft polymers can be much higher than for the other dendritic polymer families, their MWD typically remains relatively narrow ($Đ < 1.1$), and thus they are referred to as *semicontrolled dendritic structures* [96]. Synthetic schemes have been developed for the preparation of dendritic graft polymers by different methods including anionic, cationic, radical, and ring-opening polymerization. Three distinct methodologies can be distinguished in the literature, namely, divergent *grafting-onto*, divergent *grafting-from*, and convergent *grafting-through* techniques.

The divergent approach relies on successive grafting reactions starting from a linear substrate (equivalent to the core in dendrimer syntheses). In the divergent grafting-onto method, polymeric side chains are coupled with the substrate, while in the divergent grafting-from method, the side chains are grown from initiating sites on the substrate. Successive grafting reactions lead to consecutive generations of branched polymers in both cases. The convergent grafting-through methodology is a one-pot technique, whereby building blocks are produced and coupled *in situ* to yield branched structures in a single reaction step. This represents the main advantage of the grafting-through methods, in analogy to the hyperbranched polymer syntheses, as it requires less time, effort, and resources to obtain high molecular weight dendritic structures. The grafting-onto and grafting-from methods, in contrast, involve distinct steps of substrate functionalization, grafting, and product isolation for each generation.

30.4.2 Synthetic Strategies, Common Structures, and Properties

30.4.2.1 Divergent Grafting-Onto Strategy The first dendrigraft polymer syntheses were reported independently by two research groups in 1991. Gauthier and Möller [12]

developed a divergent anionic grafting-onto method for the preparation of branched PSs denominated arborescent polymers. The term *arborescent* referred to the treelike architecture of the molecules, with symmetric long branches. Tomalia et al. [13], on the other hand, employed cationic polymerization in a similar divergent grafting-onto scheme to synthesize branched polyethylenimines, initially called *Comb-burst® polymers*. The term *dendrigraft polymers* has meanwhile become widely accepted to designate arborescent, Comb-burst, and other related dendritic graft polymer architectures collectively. The divergent grafting-onto strategy is represented schematically in Figure 30.9. Specific details of the anionic and the cationic grafting methods developed by Gauthier and Möller and by Tomalia et al., respectively, are discussed in the subsequent sections.

Arborescent Polymers The first grafting technique developed for the synthesis of arborescent polymers used chloromethyl coupling sites located on the phenyl pendants of PS substrates. Coupling "living" polystyryl anions with the chloromethyl sites on the substrate thus resulted in a comb-branched, or generation 0 (G0) arborescent PS structure. Repetition of the functionalization and grafting reactions led to arborescent polymers of generations G1, G2, G3, etc. Efficient coupling with the substrate required "capping" of the living chains with a single 1,1-diphenylethylene unit to suppress metal-halogen exchange side reactions. One of the major problems encountered in this approach was associated with the use of hazardous chloromethyl methyl ether for the introduction of the chloromethyl coupling sites on the substrate. This issue was solved in 2001, when Li and Gauthier [97] developed an alternate grafting method based on acetyl coupling sites (derived from acetyl chloride). In this case, the living PS chains were capped with a few 2-vinylpyridine units before coupling with the acetylated substrate, and LiCl was added to suppress proton abstraction from the acetyl groups leading to chain termination. The synthetic paths for the preparation of G0 arborescent PS using both chloromethyl and acetyl coupling sites are compared in Scheme 30.14.

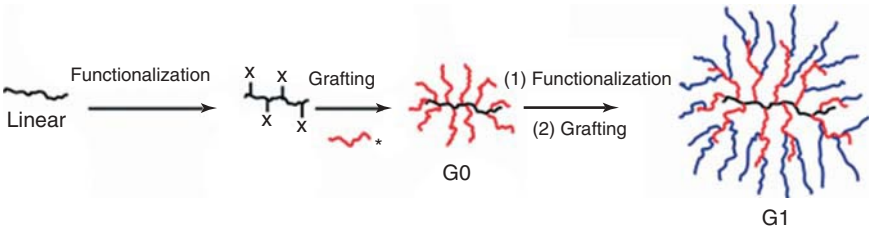

Figure 30.9 Schematic representation of the generation-based synthesis of dendrigraft polymers by a divergent *grafting-onto* method. (*See insert for the color representation of the figure*.)

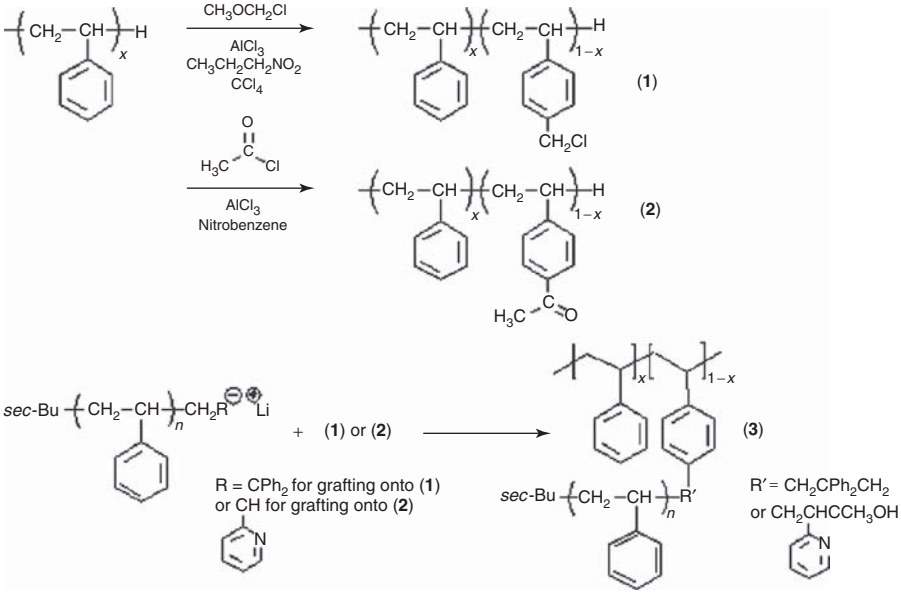

Scheme 30.14 Arborescent polystyrene synthesis: linear substrate functionalization by chloromethylation (**1**) or acetylation (**2**), and coupling with living polystyrene to yield a G0 molecule (**3**).

The scope of the grafting methods initially developed for PS was expanded over the years to the synthesis of arborescent copolymers, mainly by grafting a polymer with a different composition in the final reaction cycle. Copolymers with core–shell morphologies were thus synthesized by grafting living poly(2-vinylpyridine) (P2VP) chains onto chloromethylated or acetylated PS substrates [98, 99]. Polystyrene-*g*-polyisoprene [100] and polystyrene-*g*-poly(*tert*-butyl methacrylate) [101] copolymers were also synthesized by a similar approach. Alternatively, molecules with an inner P2VP shell embedded between a core and a corona of PS were obtained by grafting a PS-*b*-P2VP block copolymer onto arborescent PS substrates [102].

Depending on the molecular weight of the side chains and the functionalization level of the substrate used in the reaction, very high overall molecular weights can be achieved in only a few grafting cycles. If the number of coupling sites (f) available per side chain on the substrate and the molecular weight of the side chains (M_{br}) remain constant for each cycle, the molecular weight (M) of an arborescent polymer can be calculated according to the following equation:

$$M = M_{br} + M_{br}f + M_{br}f^2 + M_{br}f^3 + \cdots = \sum_{x=0}^{G+1} M_{br}f^x \tag{30.11}$$

Three key parameters characterize the success of a grafting reaction: the grafting yield (G_y), defined as the fraction of side chains generated in the reaction becoming attached on the substrate; the branching functionality (f_w), corresponding to the number of chains added in a grafting reaction; and the coupling efficiency (C_e), which is the fraction of coupling sites grafted with side chains. Arborescent polymers are typically synthesized from linear polymer building blocks having a molecular weight of about 5000 g/mol and substrates with target functionalization levels of circa 25–30 mol%. This provides a large number of coupling sites on the substrate (10–15 per side chain), while minimizing steric hindrance effects that would become more important at higher grafting densities. The grafting of coronal side chains has been investigated for both long (30,000 g/mol) and short (5000 g/mol) chain segments, resulting in either starlike or crew-cut [103] architectures, respectively. For increased side-chain lengths, the grafting yield and the coupling efficiency decrease due to enhanced steric crowding by the longer chains. The same effect also comes into play when grafting onto substrates of the upper generations. The small molecules used in the substrate functionalization process can easily diffuse on the periphery and the interior of the branched structures. The ability of polymeric chains to diffuse to the coupling sites located within the interior of the branched substrates decreases as their size increases, however, which reduces the grafting yield and the coupling efficiency. Typical values of grafting yield and coupling efficiency thus range from upward of 90% in G0 polymer syntheses, down to circa 20% for G4 polymers. Narrow MWD are maintained over successive grafting reactions, and $Đ$ sometimes even decreases marginally as a result of averaging of the side-chain length distribution. The molecular weight of these polymers can range from circa 5×10^4 g/mol for G0 to over 10^7 g/mol for G4 polymers, depending on the length of the side chains and the grafting density used in the synthesis.

The spherical topology of arborescent polymers is a consequence of the molecular weight of the polymer chains used in their synthesis: a prolate spheroid having at most a 3 : 2 axis ratio is expected for a G0 molecule (if it were to adopt a fully extended chain conformation) when grafting side chains having the same molecular weight as the linear substrate (e.g., 5000 g/mol for both components). This changes to an increasingly spherical topology over successive grafting cycles (5 : 3 axis ratio for a G1 polymer, 7 : 5 for G2, and so on). This topology is reflected in the dilute-solution properties of arborescent polymers in terms of their scaling behavior (molecular weight dependence) for the second virial coefficient (A_2), the z-average translational diffusion coefficient (D_z), and the radius of gyration (r_g), which are all comparable to rigid spheres [104]. More recently, it was shown through small-angle neutron scattering measurements that the chain segment density of arborescent polymer molecules becomes relatively constant at their center after a few grafting cycles, but decreases according to a power law within their corona [105].

Comb-burst Polymers The divergent grafting-onto method suggested by Tomalia et al. [13] for the synthesis of Comb-burst polymers yields a molecular architecture similar to the arborescent systems, but these polymers are produced through cationic polymerization of 2-ethyl-2-oxazoline. The side chains inherently contain protected coupling sites that are activated by deacylation under acidic conditions. The secondary amine sites generated along the substrate polymer can be coupled with living poly(2-ethyl-2-oxazoline) in a predetermined molar ratio to control the branching density. Another possibility is through partial deacylation of a fraction of the secondary amine sites. Depicted in Scheme 30.15 is the cationic synthesis of Comb-burst poly(2-ethyl-2-oxazoline), by initiation of the polymerization with methyl tosylate, as well as substrate activation and grafting to yield a G0 polyethylenimine (**3**).

The number of RU (N_{RU}) and the molecular weight (M) of Comb-burst polymers can be predicted from the number

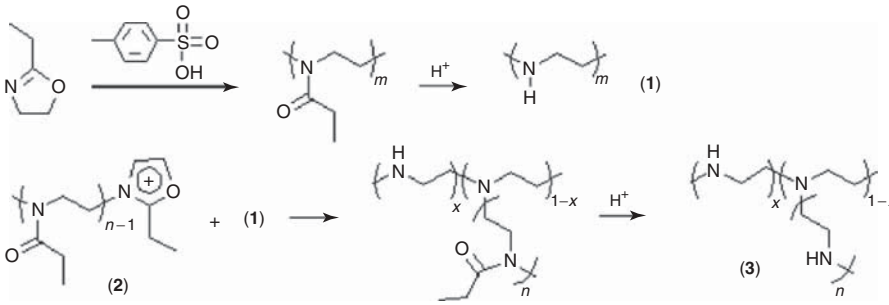

Scheme 30.15 Grafting of living poly(2-ethyl-2-oxazoline) (**2**) onto a linear polyethylenimine (**1**) to yield a G0 Comb-burst polyethylenimine (**3**).

of coupling sites on the branches (N_b) and the core (N_c), the molecular weight of the core (M_c), the molecular weight of the RU (M_{RU}), and the molecular weight of the end groups (M_z), according to the following expressions:

$$N_{RU} = N_c \left(\frac{N_b^{G+1} - 1}{N_b - 1} \right)$$

$$M = M_c + N_c \left[M_{RU} \left(\frac{N_b^{G+1} - 1}{N_b - 1} \right) + M_z N_b^{G+1} \right] \quad (30.12)$$

A series of Comb-burst polyethylenimine was thus synthesized with a side-chain DP increasing from 10 to 20 for the first two generations, and then maintained constant at 100 for the subsequent generations [106]. A geometric increase in molecular weight was observed as predicted by Equation 30.12, with grafting yield variations similar to those observed for arborescent systems.

30.4.2.2 Divergent Grafting-From Strategy In a divergent grafting-from method, polymer chains are grown from a substrate acting as a polyfunctional initiator. This approach is particularly advantageous for the preparation of copolymers with core–shell morphologies, as these can be obtained simply through the addition of different monomers in the side-chain growth process. As with the grafting-onto method, variations in the dimensions of the initiating core relatively to the side chains, as well as the location of the initiating sites, can produce different topologies. Spherical molecules result when the core has dimensions comparable to the side chains and the latter are evenly distributed around the core. If the DP of the side chains in the first grating cycle (G0 polymer synthesis) is significantly lower than that of the core, cylindrical structures will result. A G0 (comb-branched) molecule exhibiting this topology is commonly referred to as a *polymeric brush*.

The divergent grafting-from method suffers from a significant drawback in terms of structural characterization. In the grafting-onto techniques, a sample of the side chains can be removed for analysis before the grafting reaction. Unfortunately, this cannot be done in the grafting-from approaches, in analogy to hyperbranched polymer syntheses. Characterization of the side chains is only possible if they can be cleaved from the substrate after the reaction. Another drawback of this method is that it often yields broadly dispersed products, due to the increased probability of side reactions and the influence of steric hindrance resulting in the retardation of propagation for some of the chains.

This approach was first developed by Six and Gnanou for the synthesis of starlike dendritic poly(ethylene oxide) [107]. Analogous results have also been obtained using dendrimerlike multifunctional initiators [108, 109]; however, we focus on methods starting from linear macroinitiator substrates in this section. One such method was reported for the synthesis of arborescent polyglycidols, starting from a linear polyglycidol macroinitiator with anionic ring-opening polymerization [110]. The linear substrate was obtained by initiating the polymerization of glycidol acetal with potassium *tert*-butoxide, and treatments with formic acid and KOH/methanol/dioxane to deprotect the hydroxyl functionalities. The initiating sites were activated by treatment with potassium *tert*-butoxide, and glycidol acetal monomer was added to grow branches from the substrate and produce a G0 structure. Further reaction cycles led to arborescent polyglycidols of generations up to G2. The synthesis of a G0 arborescent polyglycidol starting from the polymerization of the acetal monomer is illustrated in Scheme 30.16 as an example.

Relatively low $Đ$ values were obtained in this synthesis ($Đ \approx 1.2–1.4$), albeit with MWD broadening over successive generations. Substrate activation with *tert*-butoxide targeted a 10% neutralization level, to provide adequate spacing for the side chains, but much higher branching densities (reaching 90%) were observed in practice. This is due to hopping of the potassium counterions among the hydroxyl groups on the macroinitiator substrate, leading to chain growth from most of the deprotected functional groups. Monomer conversion reached 99% during the first

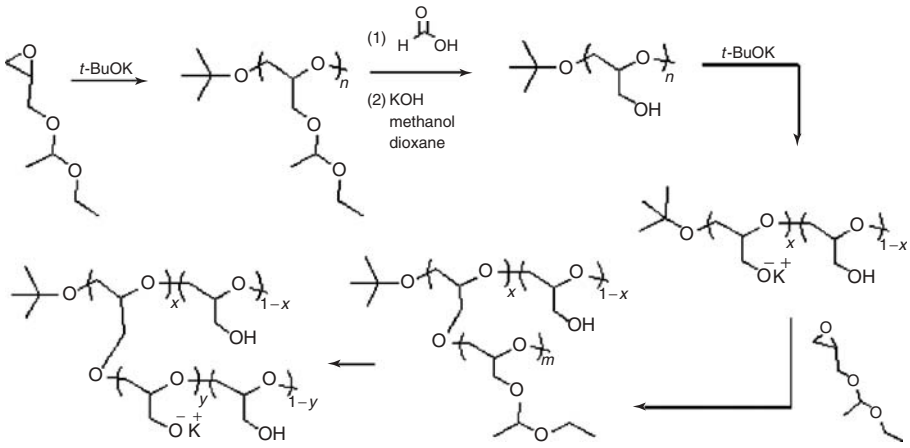

Scheme 30.16 Synthesis of a G0 arborescent polyglycidol molecule.

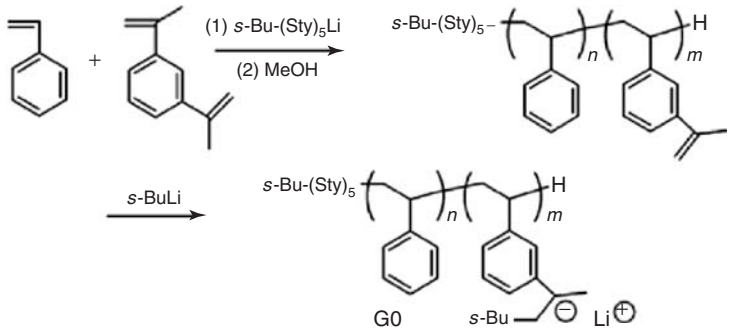

Scheme 30.17 One-pot synthesis of arborescent polystyrene by a semibatch process with mixed monomer additions. *Source*: Reproduced with permission from Yuan Z, Gauthier M. Macromolecules 2063;2006:39 [114]. Copyright 2006 American Chemical Society.

two grafting cycles, but decreased to 27% for the G2 polyglycidol due to poor solubility of the graft polymer.

An approach similar to the previous divergent grafting-from method also served to synthesize dendrigraft poly(L-lysine) by ring-opening polymerization [111], styrene homopolymers and styrene–methacrylate copolymers by a combination of stable free-radical polymerization and atom transfer radical polymerization (ATRP) [112], and copolymers of 2-hydroxyethyl methacrylate with styrene or *tert*-butyl methacrylate by ATRP [113].

Another embodiment of this technique was used for the synthesis of high molecular weight, low $Đ$ arborescent polymers by Yuan and Gauthier in a one-pot synthesis of arborescent PSs [114]. In this case, the anionic copolymerization of styrene (Sty) and 1,3-diisopropenylbenzene (DIB) initiated by *sec*-butyllithium was carried out in a semibatch process. Following complete monomer conversion, the chains were terminated and the isopropenyl moieties of the DIB units were activated with *sec*-butyllithium to produce a polyfunctional anionic macroinitiator without additional workup. Further styrene-DIB monomer mixture additions yielded a comb-branched (G0) copolymer, and subsequently G1 arborescent PS molecules after activation and styrene addition. An illustration of this synthetic technique is provided in Scheme 30.17.

Control over the side-chain molecular weight was achieved through the amount of monomer added to the activated substrates. The $Đ$ values obtained ranged from 1.1 to 1.3 for molecular weights (M_w) reaching 7×10^6 g/mol. The same technique was also used to synthesize arborescent copolymers, by adding other monomers in the last side-chain growth cycle, namely, arborescent polystyrene-*g*-poly(*tert*-butyl methacrylate) and polystyrene-*g*-[polystyrene-*b*-poly(2-vinylpyridine)] copolymers [115].

Hybrid techniques combining grafting-onto and grafting-from methodologies have also been investigated for arborescent polymer molecules, by introducing functional groups at the chain ends of an arborescent polymer and activating them to grow a corona of polymer segments with a different chemical composition [116].

30.4.2.3 Convergent Grafting-Through Strategy The convergent grafting-through method is the least time- and

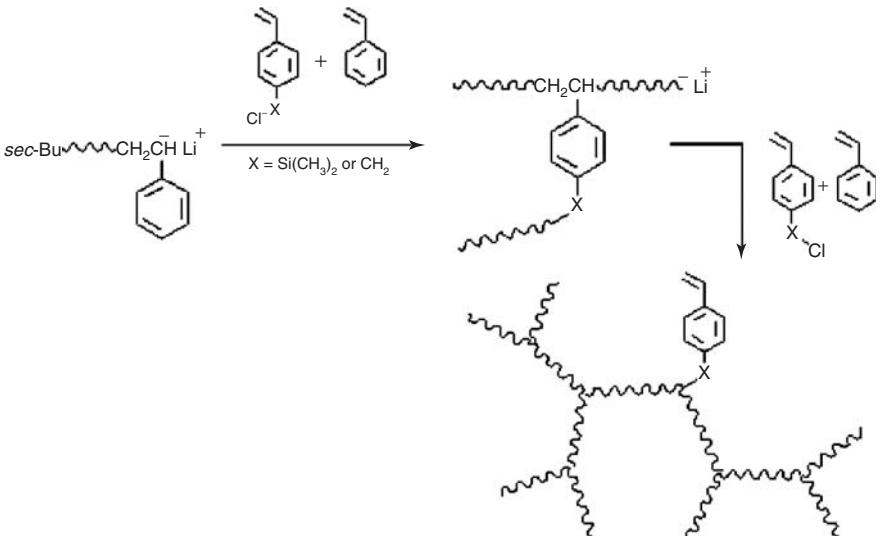

Scheme 30.18 One-pot *grafting-through* method to for the convergent synthesis of dendrigraft polystyrene.

resource-intensive approach for the synthesis of dendrigraft polymers. This self-branching system, carried in a one-pot reaction, makes use of bifunctional monomers carrying a vinyl group and a second functional group capable of coupling *in situ* with the living chains. The bifunctional monomer can be added slowly at different stages of the reaction to induce the formation of branching points, while maintaining relatively low $Đ$ typical for dendrigraft polymers.

This technique was first developed by Knauss et al. for the convergent anionic synthesis of PS. On addition of a bifunctional monomer such as 4-(chlorodimethylsilyl)styrene [117] or vinylbenzyl chloride [118] to living polystyryllithium, a portion of the living chains undergo nucleophilic substitution at their chloromethyl or chlorosilyl site, while propagation may take place via the vinyl group. The branched macromonomers generated in the coupling reaction quickly become sterically crowded, which limits the attainable molecular weight, but this growth mechanism is also believed to be at the origin of the relatively narrow MWD observed in some cases ($Đ \approx 1.1-1.8$). To facilitate the attainment of higher molecular weights and branching functionalities, styrene monomer can be added along with the bifunctional monomer to introduce PS segment spacers between the branching points, thus reducing the influence of steric crowding on the branching process. In the absence of PS spacers, the branched structures obtained are closer to star-branched polymers than to dendrigraft polymers. A polymerization process with styrene addition to produce spacers between the branching points is depicted in Scheme 30.18.

The branched structure of dendrigraft polymers obtained by the convergent grafting-through method can be described in terms of an average generation number (G) determined from Equation 30.13, where M_G and M_0 correspond to the M_n for the graft polymer and the primary chains (before addition of the coupling agent), respectively, and M_B is the molecular weight of the structural unit derived from the coupling agent:

$$G = \log\left(M_G\right) - \log\left(M_0 + M_B\right) \tag{30.13}$$

The bifunctional monomer approach, with continuous addition of the monomer and the branching agent, is analogous to hyperbranched polymer syntheses using the inimer technology, but the MWD obtained are significantly narrower: the $Đ$ values reported vary from 1.2 to 2.0, albeit the molecular weight is also limited to circa 10^5 g/mol [117, 118].

A similar approach was used to construct a unique triblock copolymer having dendritic termini connected by linear segment. The synthesis of the dendritic-*block*-linear-*block*-dendritic PS, referred to as the *pom-pom* structure due to its dumbbell-like shape, results from a convergent anionic polymerization procedure using dichlorodimethylsilane as a coupling agent [119].

30.4.3 Applications and Recent Trends

Considering the versatility of dendrigraft polymer syntheses, it is relatively easy to introduce features in the molecules of interest for specific applications. Since the chain segments of dendrigraft polymers are covalently bonded, copolymers with amphiphilic character behave like unimolecular micelles that provide an interesting basis for comparison with regular micelles. The self-assembly of

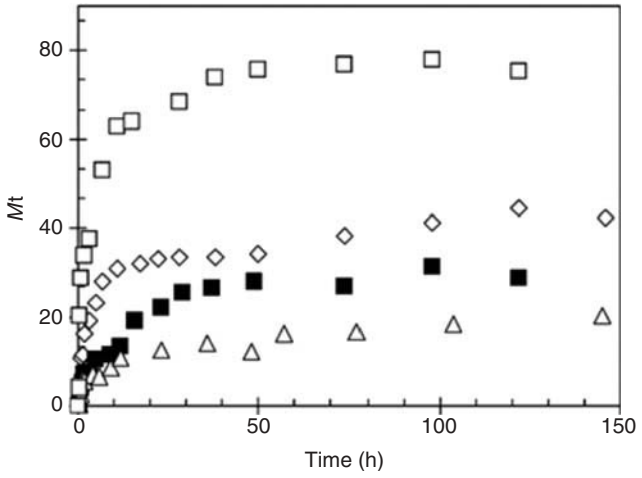

Figure 30.10 Percent mass fraction of lidocaine released from an arborescent PS-*g*-P2VP G1 (□) copolymer, and of indomethacin released from G1 (◊), G2 (■), and G3 (△) copolymers. *Source*: Reproduced with permission from Njikang GN, Gauthier M, Li J. Polymer 2008;49:5474 [120]. Copyright 2008 Elsevier.

block copolymers into micelles under selective solvency conditions is indeed concentration dependent, requiring a minimum concentration (the critical micelle concentration (CMC)), which is nonexistent for unimolecular micelles. Thus, depending on the specific application targeted, the dynamic character of block copolymer assemblies and their sensitivity to solvency conditions may be problematic, for example, when trying to load host molecules within their core.

The core–shell morphology of amphiphilic dendrigraft polymers, and the ability to control their characteristics (hydrophobic core size, hydrophilic corona thickness) independently, provides a wider range of structures than can be achieved for block copolymer micelles. A good example of this is arborescent amphiphiles incorporating a hydrophobic arborescent PS core and a corona of polar P2VP segments [98, 99]. These copolymers are interesting in terms of their solubilization properties [99] and their ability to host and slowly release hydrophobic compounds [120]. *In vitro* loading and release studies of indomethacin and lidocaine from PS-*g*-P2VP arborescent copolymers of different generations showed that the release profiles for the model drugs displayed an initial burst release, followed by more gradual release over extended time periods. The release profiles obtained for indomethacin and lidocaine from different host PS-*g*-P2VP copolymers are compared in Figure 30.10 as an example.

It is clear from Figure 30.10 that the release from upper generation copolymers is more gradual, which can be attributed to the increased branching functionality of the molecules. It should also be noted that ionic interactions are present between the carboxylic acid group of the drug and the nitrogen atom of the pyridine pendants, which explains the much slower overall release rate for indomethacin as compared to lidocaine.

The usefulness of analogous arborescent copolymers characterized by a layered architecture, with an inner shell of P2VP segments, has been recently demonstrated as unimolecular templates for the preparation of metallic nanoparticles in nonpolar solvents [102]. Metallic nanoparticles are being intensively investigated for applications including imaging agents, microelectronics, separation science, catalysis, and biological uses such as targeted labeling and delivery systems or cell therapy. Arborescent copolymers with reverse micelle characteristics are obtained by grafting living PS-*b*-P2VP block copolymers onto arborescent PS substrates according to the methods described previously [12, 97]. A schematic representation of the synthesis of a template molecule, its loading with a metallic salt, and the reduction of the salt to metallic nanoparticles is shown in Figure 30.11. Since the living end of the block copolymer serving as side-chains is located at the end of the P2VP segment, a core–shell–corona copolymer architecture is obtained, with a corona of PS chains providing compatibility with nonpolar organic solvents, an inner shell of P2VP, and a PS core. The P2VP shell enables the loading of polar compounds, for example, through coordination with transition metals or, for charged species, through ionic interactions. This templating approach to the preparation of metallic nanoparticles has so far been explored using $HAuCl_4$.

The metals loaded in the arborescent templates may be easily viewed by transmission electron microscopy (TEM) as shown in Figure 30.12 [102]. The generation number of the PS-*g*-(P2VP-*b*-PS) templates governs the distribution of the metallic species within the molecules: the G0 templates (Fig. 30.12a), having an ill-defined core comprised of a

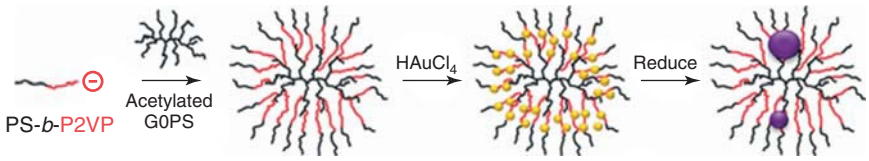

Figure 30.11 Synthesis of an arborescent copolymer, G0PS-*g*-(P2VP-*b*-PS), its application to templating $HAuCl_4$ deposition, and reduction to gold nanoparticles. (*See insert for the color representation of the figure*.)

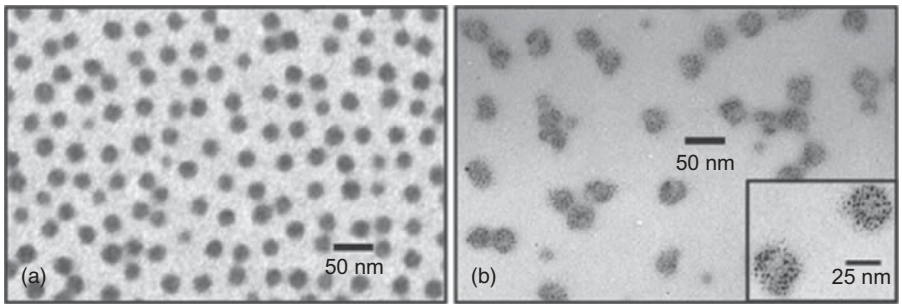

Figure 30.12 TEM micrographs for (a) PS-*g*-(P2VP-*b*-PS) and (b) G1PS-*g*-(P2VP-*b*-PS) loaded with $HAuCl_4$; the high magnification inset depicts the ring-like arrangement of Au. *Source*: Reproduced with permission from Dockendorff J, Gauthier M, Mourran A, Möller M. Macromolecules 2008;41:6621 [102]. Copyright 2008 American Chemical Society.

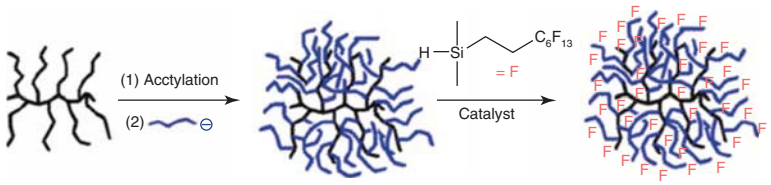

Scheme 30.19 Synthesis of G0PS-*g*-PIP copolymer followed by hydrosilation with a fluorohydrosilane for use as a processing aid. *Source*: Reproduced with permission from Gauthier M, Lin W–Y, Teertstra SJ, Tzoganakis C. Polymer 2010;51:3123 [121]. Copyright 2010 Elsevier. (*See insert for the color representation of the figure*.)

single linear PS chain, provide a uniform distribution of gold, while the G2 species (Fig. 30.12b), incorporating a larger noncoordinating G1PS core, display a metal-depleted region at the center of the nanoparticles.

The high molecular weight, compact structure, and spherical topology of arborescent polymers confer them a low viscosity as compared to their linear counterparts. These characteristics are also attractive for their potential application as polymer processing additives. It has indeed been demonstrated that branched polymers with a high degree of symmetry have a greater tendency to diffuse to the surface of polymer blends [121], and so they can interact more efficiently with the die wall surface and modify the processing characteristics of the host polymer. Linear fluoroelastomers have been instated as polymer processing additives for many years due to their ability to induce slippage at the walls of processing equipment, which leads to reduced melt defects and energy consumption. For that reason, fluorine-containing arborescent polystyrene-*g*-polyisoprene copolymers, combining the inherent properties of branched polymers with the surface energy reduction of fluorinated polymers, have been investigated as processing aids [121]. Arborescent copolymers with a PS core and polyisoprene (PIP) side chains were synthesized by a divergent grafting-onto method [97] and hydrosilylated with a fluorohydrosilane as depicted in Scheme 30.19.

Capillary rheometer extrusion tests were performed by monitoring the applied pressure and the extrudate appearance as a function of the deformation (shear) rate, for blends of the arborescent copolymers at 0.5% w/w with a commercial linear low density polyethylene (LLDPE) resin. In all cases, the backpressure was reduced for the blends as compared to virgin LLDPE; however, the performance of the arborescent additives was inferior to a commercial additive used for comparison.

30.5 CONCLUDING REMARKS

The dendritic polymer literature reviewed herein provides compelling evidence that these materials are a unique and versatile class of branched polymers. The synthesis of dendritic macromolecules can be accomplished by numerous methods allowing for specific tailoring of the characteristics of the polymer, to yield desired properties or functionality. While some of the procedures reported are quite intricate, requiring multiple cycles of synthetic steps and work-up, one-pot syntheses have also been developed for hyperbranched and dendrigraft polymers, making these materials more viable for (large-scale) commercial production and industrial applications.

The low viscosity [122] of dendritic polymers is interesting in terms of their potential applications as rheological (or

viscosity) modifiers and/or as polymer processing aids. Furthermore, the multiple chemical functionalities available for these materials offers a wide range of applications in different areas including stabilized catalysts, biological markers, sensors, and micelle mimics.

Dendritic polymers have been the focus of a great deal of application-oriented research in recent years. The number of U.S. patents related to dendritic polymers issued between 1990 and 1999 totaled 62, and only three patents were issued before 1990. From 2000 until July 2010, approximately 240 additional dendrimer-related patents were issued, that is almost four times the number issued in the previous decade.[1] The number of patent applications relating to dendritic species over the same period totaled approximately 430, demonstrating that this field is receiving even more attention than the number of already issued patents suggests. Recent emphasis on more exotic applications within the fields of nanotechnology, pharmaceuticals, and biotechnology has resulted in rapid growth in the number of filings. Further investigation into these fields as well as the new synthetic approaches and hybrid methodologies being developed will certainly broaden the scope of dendritic polymer applications in the future.

REFERENCES

1. Buhleier E, Wehner W, Vögtle F. Synthesis 1978;2:155.
2. Tomalia DA, Fréchet JMJ. J Polym Sci A Polym Chem 2002;40:2719.
3. Maciejewski M. J Macromol Sci Pure Appl Chem 1982;17:689.
4. de Gennes PG, Hervet H. J Physique Lett 1983;44:L-351.
5. Tomalia DA, Baker H, Dewald J, Hall M, Kallos G, Martin S, Roeck J, Ryder J, Smith P. Polym J 1985;17:117.
6. Newkome GR, Yao Z-q, Baker GR, Gupta VK. J Org Chem 1985;50:2003.
7. Hawker CJ, Fréchet JMJ. J Am Chem Soc 1990;112:7638.
8. Miller TM, Neenan TX. Chem Mater 1990;2:346.
9. Gunatillake PA, Odian G, Tomalia DA. Macromolecules 1988;21:1556.
10. Kim YH, Webster OW. J Am Chem Soc 1990;112:4592.
11. Hawker CJ, Lee R, Fréchet JMJ. J Am Chem Soc 1991;113:4583.
12. Gauthier M, Möller M. Macromolecules 1991;24:4548.
13. Tomalia DA, Hedstrand DM, Ferritto MS. Macromolecules 1991;24:1435.
14. Tomalia DA, Fréchet JMJ. Introduction to the dendritic state. In: Tomalia DA, Fréchet JMJ, editors. *Dendrimers and Other Dendritic Polymers*. West Sussex: Wiley; 2001. p 3.
15. Tomalia DA, Berry V, Hall M, Hedstrand DM. Macromolecules 1987;20:1164.
16. Naylor AM, Goddard WA III,, Kiefer GE, Tomalia DA. J Am Chem Soc 1989;111:2339.
17. Wörner C, Mülhaupt R. Angew Chem Int Ed Engl 1993;32:1306.
18. de Brabander-van den Berg EMM, Meijer EW. Angew Chem Int Ed Engl 1993;32:1308.
19. Inoue K. Prog Polym Sci 2000;25:453.
20. Zhao M, Sun L, Crooks RM. J Am Chem Soc 1998;120:4877.
21. Balogh L, Tomalia DA. J Am Chem Soc 1998;120:7355.
22. Gröhn F, Bauer BJ, Akpalu YA, Jackson CL, Amis EJ. Macromolecules 2000;33:6042.
23. Scott RWJ, Ye H, Henriquez RR, Crooks RM. Chem Mater 2003;15:3873.
24. Gu Y, Xie H, Gao J, Liu D, Williams CT, Murphy CJ, Ploehn HJ. Langmuir 2005;21:3122.
25. Peng Z, Zhang J, Sun X, Yang J, Diao J. Colloid Polym Sci 2009;287:609.
26. Atwater JE, Akse JR, Holtsnider JT. Mater Lett 2008;62:3131.
27. Scott RWJ, Wilson OM, Oh S-K, Kenik EA, Crooks RM. J Am Chem Soc 2004;126:15583.
28. Gu Y, Wu G, Hu XF, Chen DA, Hansen T, zur Loye H-C, Ploehn HJ. J Power Sources 2010;195:425.
29. Newkome GR, He E, Moorefield CN. Chem Rev 1999;99:1689.
30. Cuadrado I, Morán M, Casado CM, Alonso B, Losada J. Coord Chem Rev 1999;193–195:395.
31. Berger A, Gebbink RJMK, van Koten G. Top Organomet Chem 2006;20:1.
32. [a] Ribaudo F, van Leeuwen PWNM, Reek JNH. Top Organomet Chem 2006;20:39. [b] King ASH, Twyman LJ. J Chem Soc Perkin Trans 1 2002:2209. [c] van Heerbeek R, Kamer PCJ, van Leeuwen PWNM, Reek JNH. Chem Rev 2002;102:3717.
33. Knapen JWJ, van der Made AW, de Wilde JC, van Leeuwen PWNM, Wijkens P, Grove DM, van Koten G. Nature 1994;372:659.
34. Reetz MT, Lohmer G, Schwickardi R. Angew Chem Int Ed Engl 1997;36:1526.
35. Bourque SC, Maltais F, Xiao W-J, Tardif O, Alper H, Arya P, Manzer LE. J Am Chem Soc 1999;121:3035.
36. Oosterom GE, van Haaren RJ, Reek JNH, Kamer PCJ, van Leeuwen PWNM. Chem Commun 1999:1119.
37. Albrecht M, Hovestad NJ, Boersma J, van Koten G. Chem Eur J 2001;7:1289.
38. Fischer M, Vögtle F. Angew Chem Int Ed 1999;38:884.
39. Navarro G, de ILarduya CT. Nanomedicine 2009;5:287.

[1]Note: Patent search results from an "advanced search" performed at http://patft.uspto.gov/ on July 13, 2010. Query included appropriate Issue Date and keyword search of "dendrimer or arborescent or dendrigraft or hyperbranched" within the abstract. An example of a query string was as follows: ISD/1/1/2000->7/13/2010 and ABST/(dendrimer or arborescent or dendrigraft or hyperbranched).

40. Bielinska A, Kukowska-Latallo JF, Johnson J, Tomalia DA, Baker JR Jr,. Nucleic Acids Res 1996;24:2176.
41. Jansen JFGA, Meijer EW, de Brabander-van den Berg EMM. J Am Chem Soc 1995;117:4417.
42. [a] Malik N, Evagorou EG, Duncan R. Anticancer Drugs 1999;10:767. [b] Howell BA, Fan D. Proc Math Phys Eng Sci 2010;466:1515.
43. Cheng Y, Li M, Xu T. Eur J Med Chem 2008;43:1791.
44. Shaunak S, Thomas S, Gianasi E, Godwin A, Jones E, Teo I, Mireskandari K, Luthert P, Duncan R, Patterson S, Khaw P, Brocchini S. Nat Nanobiotechnol 2004;22:977.
45. [a] Nantalaksakul A, Reddy DR, Bardeen CJ, Thayumanavan S. Photosynth Res 2006;87:133. [b] Adronov A, Fréchet JMJ. Chem Commun 2000:1701. [c] Devadoss C, Bharathi P, Moore JS. J Am Chem Soc 1996;118:9635. [d] Lo S-C, Burn PL. Chem Rev 2007;107:1097.
46. Flory PJ. J Am Chem Soc 1952;74:2718.
47. Yan D, Müller AHE, Matyjaszewski K. Macromolecules 1997;30:7024.
48. Hölter D, Burgath A, Frey H. Acta Polym 1997;48:30.
49. Erlander S, French D. J Polym Sci 1956;20:7.
50. Burchard W. Macromolecules 1972;5:604.
51. Hanselmann R, Hölter D, Frey H. Macromolecules 1998;31:3790.
52. Bharathi P, Moore JS. Macromolecules 2000;33:3212.
53. Gong C, Miravet J, Fréchet JMJ. J Polym Sci A Polym Chem 1999;37:3193.
54. Schallausky F, Erber M, Komber H, Lederer A. Macromol Chem Phys 2008;209:2331.
55. Radke W, Litvinenko G, Müller AHE. Macromolecules 1998;31:239.
56. Yan D, Zhou Z, Müller AHE. Macromolecules 1999;32:245.
57. Gao C, Yan D. Prog Polym Sci 2004;29:183.
58. Miller TM, Neenan TX, Kwock EW, Stein SM. J Am Chem Soc 1993;115:356.
59. Wooley KL, Hawker CJ, Lee R, Fréchet JMJ. Polym J 1994;26:187.
60. Spindler R, Fréchet JMJ. Macromolecules 1993;26:4809.
61. Mathias LJ, Carothers TW. J Am Chem Soc 1991;113:4043.
62. Bolton DH, Wooley KL. Macromolecules 1890;1997:30.
63. Yoon K, Son DY. Macromolecules 1999;32:5210.
64. Miravet JF, Fréchet JMJ. Macromolecules 1998;31:3461.
65. Hawker CJ, Fréchet JMJ, Grubbs RB, Dao J. J Am Chem Soc 1995;117:10763.
66. Fréchet JMJ, Henmi M, Gitsov I, Aoshima S, Leduc MR, Grubbs RB. Science 1995;269:1080.
67. [a] Paulo C, Puskas JE. Macromolecules 2001;34:734. [b] Puskas JE, Dos Santos LM, Kaszas G, Kulbaba K. J Polym Sci A Polym Chem 2009;47:1148.
68. Foreman EA, Puskas JE, Kaszas G. J Polym Sci A Polym Chem 2007;45:5847.
69. Liu M, Vladimirov N, Fréchet JMJ. Macromolecules 1999;32:6881.
70. Sunder A, Hanselmann R, Frey H, Mülhaupt R. Macromolecules 1999;32:4240.
71. Magnusson H, Malmström E, Hult A. Macromol Rapid Commun 1999;20:453.
72. Suzuki M, Ii A, Saegusa T. Macromolecules 1992;25:7071.
73. Jikei M, Chon S-H, Kakimoto M-a, Kawauchi S, Imase T, Watanebe J. Macromolecules 1999;32:2061.
74. Emrick T, Chang H-T, Fréchet JMJ. Macromolecules 1999;32:6380.
75. Tanaka S, Takeuchi K, Asai M, Iso T, Ueda M. Synth Met 2001;119:139.
76. Mendez JD, Schroeter M, Weder C. Macromol Chem Phys 2007;208:1625.
77. Pérignon N, Mingotaud A-F, Marty J-D, Rico-Lattes I, Mingotaud C. Chem Mater 2004;16:4856.
78. Salazar R, Fomina L, Fomine S. Polym Bull 2001;47:151.
79. Slagt MQ, Stiriba S-E, Klein Gebbink RMJ, Kautz H, Frey H, van Koten G. Macromolecules 2002;35:5734.
80. Slagt MQ, Stiriba S-E, Kautz H, Klein Gebbink RJM, Frey H, van Koten G. Organometallics 2004;23:1525.
81. Krämer M, Pérignon N, Haag R, Marty J-D, Thomann R, Lauth-de Viguerie N, Mingotaud C. Macromolecules 2005;38:8308.
82. Yang J, Lin H, He Q, Ling L, Zhu C, Bai F. Langmuir 2001;17:5978.
83. Lee J-C, Lee W, Han S-H, Kim TG, Sung Y-M. Electrochem Commun 2009;11:231.
84. Häußler M, Lam JWY, Zheng R, Dong H, Tong H, Tang BZ. J Inorg Organomet Polym Mater 2005;15:519.
85. Onitsuka K, Ohshiro N, Fujimoto M, Takei F, Takahashi S. Mol Cryst Liq Cryst 2000;342:159.
86. Hagihara N, Sonogashira K, Takahashi S. Adv Polym Sci 1981;41:149.
87. Takahashi S, Onitsuka K, Takei F. Macromol Symp 2000;156:69.
88. Frey H, Haag R. Rev Mol Biotechnol 2002;90:257.
89. Cosulich ME, Russo S, Pasquale S, Mariani A. Polymer 2000;41:4951.
90. Boulares-Pender A, Prager-Duschke A, Elsner C, Buchmeiser MR. J Appl Polym Sci 2009;112:2701.
91. Muthukrishnan S, Nitschke M, Gramm S, Özyürek Z, Voit B, Werner C, Müller AHE. Macromol Biosci 2006;6:658.
92. Puskas JE, Dos Santos LM, Fischer F, Götz C, El Fray M, Altstädt V, Tomkins M. Polymer 2009;50:591.
93. Puskas JE, Chen Y, Dahman Y, Padavan D. J Polym Sci A Polym Chem 2004;42:3091.
94. [a] Puskas JE, Chen Y, Antony P, Kwon Y, Kovar M, Harbottle RR, De Jong K, Norton PR, Cadieux P, Burton J, Reid G, Beiko D, Watterson JD, Denstedt J. Polym Adv Technol 2003;14:763. [b] Foreman E, Puskas JE, El Fray M, Prowans P, Piątek M. Polym Prepr 2008;49(1):822.
95. Cadieux P, Watterson JD, Denstedt J, Harbottle RR, Puskas J, Howard J, Gan BS, Reid G. Colloids Surf B Biointerfaces 2003;28:95.

96. Kee RA, Gauthier M, Tomalia DA. Semi-controlled dendritic structure synthesis. In: Tomalia DA, Fréchet JMJ, editors. *Dendrimers and Other Dendritic Polymers*. West Sussex: Wiley; 2001. p 209.
97. Li J, Gauthier M. Macromolecules 2001;34:8918.
98. Kee RA, Gauthier M. Macromolecules 2002;35:6526.
99. Gauthier M, Li J, Dockendorff J. Macromolecules 2003;36:2642.
100. Kee RA, Gauthier M. Macromolecules 1999;32:6478.
101. Kee RA, Gauthier M. J Polym Sci A Polym Chem 2008;46:2335.
102. Dockendorff J, Gauthier M, Mourran A, Möller M. Macromolecules 2008;41:6621.
103. Zhang L, Eisenberg A. J Am Chem Soc 1996;118:3168.
104. Gauthier M, Möller M, Burchard W. Macromol Symp 1994;77:43.
105. Il Yun S, Lai K-C, Briber RM, Teertstra SJ, Gauthier M, Bauer BJ. Macromolecules 2008;41:175.
106. Yin R, Swanson DR, Tomalia DA. Polym Mater Sci Eng 1995;73:277.
107. Six J-L, Gnanou Y. Macromol Symp 1995;95:137.
108. Hirao A, Sugiyama K, Tsunoda Y, Matsuo A, Watanabe T. J Polym Sci A Polym Chem 2006;44:6659.
109. Trollsås M, Hedrick JL. J Am Chem Soc 1998;120:4644.
110. Walach W, Kowalczuk A, Trzebicka B, Dworak A. Macromol Rapid Commun 2001;22:1272.
111. Klok H-A, Rodríguez-Hernández J. Macromolecules 2002;35:8718.
112. Grubbs RB, Hawker CJ, Dao J, Fréchet JMJ. Angew Chem Int Ed Engl 1997;36:270.
113. Cheng G, Böker A, Zhang M, Krausch G, Müller AHE. Macromolecules 2001;34:6883.
114. Yuan Z, Gauthier M. Macromolecules 2063;2006:39.
115. Yuan Z, Gauthier M. Macromol Chem Phys 2007;208:1615.
116. Gauthier M, Tichagwa L, Downey JS, Gao S. Macromolecules 1996;29:519.
117. Knauss DM, Al-Muallem HA, Huang T, Wu DT. Macromolecules 2000;33:3557.
118. Knauss DM, Al-Muallem HA. J Polym Sci A Polym Chem 2000;38:4289.
119. Knauss DM, Huang T. Macromolecules 2055;2002:35.
120. Njikang GN, Gauthier M, Li J. Polymer 2008;49:5474.
121. Gauthier M, Lin W-Y, Teertstra SJ, Tzoganakis C. Polymer 2010;51:3123.
122. Puskas JE, Kaszas G. Prog Polym Sci 2000;25:403.